



HAL
open science

Mathematical analysis of a three-tiered model of anaerobic digestion

Sarra Nouaoura, Nahla Abdellatif, Radhouane Fekih-Salem, Tewfik Sari

► **To cite this version:**

Sarra Nouaoura, Nahla Abdellatif, Radhouane Fekih-Salem, Tewfik Sari. Mathematical analysis of a three-tiered model of anaerobic digestion. 2020. hal-02540350v2

HAL Id: hal-02540350

<https://hal.science/hal-02540350v2>

Preprint submitted on 17 Jul 2020 (v2), last revised 12 Jan 2021 (v3)

HAL is a multi-disciplinary open access archive for the deposit and dissemination of scientific research documents, whether they are published or not. The documents may come from teaching and research institutions in France or abroad, or from public or private research centers.

L'archive ouverte pluridisciplinaire **HAL**, est destinée au dépôt et à la diffusion de documents scientifiques de niveau recherche, publiés ou non, émanant des établissements d'enseignement et de recherche français ou étrangers, des laboratoires publics ou privés.

MATHEMATICAL ANALYSIS OF A THREE-TIERED MODEL OF ANAEROBIC DIGESTION *

SARRA NOUAOURA[†], NAHLA ABDELLATIF[‡], RADHOUANE FEKIH-SALEM[§], AND TEWFIK SARI[¶]

Abstract. In this paper, we are interested in a mechanistic model describing the anaerobic mineralization of chlorophenol in a three-step food-web. The model is a six-dimensional system of ordinary differential equations. In our study, we take into account the phenol and the hydrogen input concentrations as well as the maintenance terms. Moreover, we consider the case of a large class of growth rates, instead of specific kinetics. In this general case, a recent study shows that the system can have up to eight steady states and their existence conditions were analytically determined. We focus here on the necessary and sufficient conditions of the local stability of the steady states, according to the four operating parameters of the process, which are the dilution rate and the chlorophenol, phenol and hydrogen input concentrations. In previous studies, this stability analysis was performed only numerically. We show that the positive steady state can be unstable and we give numerical evidence for a supercritical Hopf bifurcation with the appearance of a stable periodic orbit. We give a bifurcation diagram with the chlorophenol input concentration as the bifurcating parameter, showing that the system can present rich behavior including bistability, coexistence and occurrence of limit cycle.

Key words. Anaerobic digestion, Bistability, Chemostat, Chlorophenol mineralization, Hopf bifurcation, Limit cycle.

AMS subject classifications. 34A34, 34D20, 37N25, 92B05

1. Introduction. The anaerobic digestion is a natural process in which organic material is converted into biogas in an environment without oxygen by the action of a microbial ecosystem. It is used for the treatment of wastewater and has the advantage of producing methane and hydrogen under appropriate conditions [12]. The removed carbon dioxide can be used as a carbon source for microalgae [11]. The full Anaerobic Digestion Model No.1.(ADM1) [1] is highly parameterized with a large number of state variables. Whilst suitable for dynamic simulation, analytical results on the model are impossible and only numerical investigations are available [4]. Due to the analytical intractability of the full ADM1, simpler mechanistic models of microbial interaction have been proposed in view of a better understanding of the anaerobic digestion process.

The two-tiered models, which take the form of four-dimensional mathematical models with a cascade of two biological reactions, where one substrate is consumed by one microorganism in a chemostat to produce a product that serves as the main limiting substrate for a second microorganism, are the simplest models which encapsulate the essence of the anaerobic digestion process. Two-tiered models with commensalistic relationship including or not substrate inhibition of the second population are widely considered [2, 3, 16, 20] where the second population (the commensal popula-

*Submitted to the editors 2020-07-17.

Funding: This work was supported by the Euro-Mediterranean research network TREASURE (<http://www.inra.fr/treasure>).

[†]University of Tunis El Manar, National Engineering School of Tunis, LAMSIN, 1002, Tunis, Tunisia (sarra.nouaoura@enit.utm.tn).

[‡]University of Manouba, National School of Computer Science, 2010, Manouba, Tunisia (nahla.abdellatif@ensi-uma.tn).

[§]University of Monastir, Higher Institute of Computer Science of Mahdia, 5111, Mahdia, Tunisia (radhouene.fekihsaleem@isima.rnu.tn).

[¶]ITAP, Univ Montpellier, INRAE, Institut Agro, Montpellier, France (tewfik.sari@inrae.fr).

tion) benefits for its growth from the first population (the host population) while the host population is not affected by the growth of the commensal population. On the contrary, when the growth of the first population is affected by the growth of the second population, the system describes a syntrophic relationship [5, 6, 8, 17, 18, 23, 27]. For more details and informations on commensalism and syntrophy, the reader is referred to [18] and the references therein. Important and interesting extensions of the two-tiered models are the eight-dimensional mathematical models, which include syntrophy and inhibition [25, 26] and the model with five state variables studied in [4, 14].

In this paper, we consider another extension of two-tiered models which consists in a six-dimensional mathematical model obtained by introducing an additional microorganism and substrate into a two-tiered syntrophic model. The organisms involved in the resulting three-tiered food-web are the chlorophenol and the phenol degraders and the hydrogenotrophic methanogen [24] (see section 4 for the description of this food-web). It has been shown in [24] that this model can have up to eight steady states. Arguing that the Routh–Hurwitz theorem allowing for an explicit analysis of the stability of steady states, is intractable beyond five dimensions, as it was noticed in [13], the stability of the steady states were determined only numerically [24] using specific growth rates (see formulas (4.2)). Several operating diagrams, which are the bifurcation diagrams with respect to the four operating parameters (i.e. the dilution rate, the chlorophenol, the phenol and the hydrogen input concentrations) have been numerically constructed in [24], showing the role, and the importance of each operating parameter, in particular for the coexistence of all three species.

The model of [24] is extended in [15, 19] with general growth rates (see section 2 for the assumptions on the growth rates) and takes the form:

$$(1.1) \quad \begin{cases} \dot{x}_0 &= (\mu_0(s_0, s_2) - D - a_0)x_0 \\ \dot{x}_1 &= (\mu_1(s_1, s_2) - D - a_1)x_1 \\ \dot{x}_2 &= (\mu_2(s_2) - D - a_2)x_2 \\ \dot{s}_0 &= D(s_0^{\text{in}} - s_0) - \mu_0(s_0, s_2)x_0 \\ \dot{s}_1 &= D(s_1^{\text{in}} - s_1) + \mu_0(s_0, s_2)x_0 - \mu_1(s_1, s_2)x_1 \\ \dot{s}_2 &= D(s_2^{\text{in}} - s_2) - \omega\mu_0(s_0, s_2)x_0 + \mu_1(s_1, s_2)x_1 - \mu_2(s_2)x_2 \end{cases}$$

where s_0 is the first substrate (chlorophenol in the application) concentration and x_0 its degrader concentration; s_1 and x_1 for the second substrate (phenol); s_2 and x_2 for the third substrate (hydrogen); D is the dilution rate; μ_i is the specific growth rate; s_i^{in} is the input substrate concentration in the chemostat; ω is a yield coefficient; a_i is the maintenance (or decay) rate for $i = 0, 1, 2$ and corresponding to chlorophenol, phenol and hydrogen, respectively. In the resulting three-tiered model (1.1), the chlorophenol degrader grows on both chlorophenol and hydrogen and produces phenol. The phenol degrader consumes the phenol to form hydrogen, which inhibits its growth. The hydrogenotrophic methanogen grows on the produced hydrogen.

The mathematical analysis of (1.1), under various assumptions, is given in [15, 19]. The system (1.1) was studied in [19] in the case $s_0^{\text{in}} > 0$ and $s_1^{\text{in}} = s_2^{\text{in}} = 0$ where at most three types of steady states can exist. The results of [19] were extended in [15] in the case $s_1^{\text{in}} \geq 0$ and $s_2^{\text{in}} \geq 0$ where at most eight types of steady states can exist. These steady states, which were depicted only numerically in [24], are analytically studied in [15, 19], providing their necessary and sufficient conditions of existence, and showing their uniqueness, except for one of them, that can exist in two forms, a fact that was not described in [24]. In [15, 19], the stability of steady states was analytically characterized only in the case without maintenance, where the

six-dimensional mathematical model is reduced to a three-dimensional one. It has been shown in [15, 19] that the positive steady state can be unstable, a fact that has also not been described in [24]. Numerical analysis has suggested the presence of a Hopf bifurcation emerging through the positive steady state, with the chlorophenol input concentration as the bifurcating parameter.

In [7], the three-tiered model of [24] was simplified by neglecting the part of hydrogen produced by the phenol degrader. The existence and stability of steady states were analytically studied only in the case without maintenance. In [22], persistence results were given in the case without maintenance, and the Hopf bifurcation of the positive steady state, which was numerically observed in [19], is proved.

Here, we focus on the analysis of the stability of all steady states of (1.1), and we analytically characterize the stability, by using the Liénard-Chipart stability criteria, in the case including maintenance, where the system cannot be reduced to a three-dimensional one. We generalize then [24] by allowing a larger class of growth functions and by giving rigorous proofs for the results on the existence and stability of steady states. For this class of growth function, we generalize [7, 15, 19, 22] by giving the necessary and sufficient conditions of stability of steady states when maintenance is included in the model.

This paper is organized as follows: in section 2, we recall the results of [15] on the existence of the steady states. We give in section 3 our main result providing the necessary and sufficient conditions of stability of the steady states. Next, in section 4, we give an application of our theoretical results to the three-tiered model considered in [24]. We dedicate section 5 to discuss our results. In Appendix A, we define some auxiliary functions used for the description of the steady states with their conditions of existence and stability. Proofs are reported in Appendix B. In Appendix C, the description of the bifurcation diagram according to the chlorophenol input concentration is supported by numerical experimentation. In Appendix D, we present the Liénard-Chipart stability criteria. Details and complements on the three-tiered model considered in [24] are given in Appendix E. In Appendix F, we illustrate some numerical simulations and some tables are given in Appendix G.

2. Assumptions and existence of steady states. We consider model (1.1). Following [15, 19], we assume that the growth functions are continuously differentiable (C^1) and satisfy the following conditions:

(H1) For all $s_0 > 0$ and $s_2 > 0$, $0 < \mu_0(s_0, s_2) < +\infty$, $\mu_0(0, s_2) = 0$, $\mu_0(s_0, 0) = 0$.

(H2) For all $s_1 > 0$ and $s_2 \geq 0$, $0 < \mu_1(s_1, s_2) < +\infty$, $\mu_1(0, s_2) = 0$.

(H3) For all $s_2 > 0$, $0 < \mu_2(s_2) < +\infty$, $\mu_2(0) = 0$.

(H4) For all $s_0 > 0$ and $s_2 > 0$, $\frac{\partial \mu_0}{\partial s_0}(s_0, s_2) > 0$, $\frac{\partial \mu_0}{\partial s_2}(s_0, s_2) > 0$.

(H5) For all $s_1 > 0$ and $s_2 > 0$, $\frac{\partial \mu_1}{\partial s_1}(s_1, s_2) > 0$, $\frac{\partial \mu_1}{\partial s_2}(s_1, s_2) < 0$.

(H6) For all $s_2 > 0$, $\mu_2'(s_2) > 0$.

(H7) The function $s_2 \mapsto \mu_0(+\infty, s_2)$ is monotonically increasing and the function $s_2 \mapsto \mu_1(+\infty, s_2)$ is monotonically decreasing.

(H8) When $\omega < 1$, the function Ψ has a unique minimum $\bar{s}_2 = \bar{s}_2(D)$ on the interval (s_2^0, s_2^1) , such that $\frac{\partial \Psi}{\partial s_2}(s_2, D) < 0$ on (s_2^0, \bar{s}_2) and $\frac{\partial \Psi}{\partial s_2}(s_2, D) > 0$ on (\bar{s}_2, s_2^1) .

Notice that the function Ψ considered in (H8), together with all other auxiliary functions needed in the following results are defined in Appendix A. We begin by recalling the main result of [15], see Theorem 1 in [15].

Theorem 2.1. Assume that Hypotheses (H1) to (H6) hold. System (1.1) can have at most eight types of steady states whose components are given in Table 1. Assume also that Hypothesis (H7) holds. The necessary and sufficient conditions of existence

of the steady states are given in [Table 2](#). When they exist, all steady states, except SS4, are unique.

- If $\omega \geq 1$, when it exists, SS4 is unique.
- If $\omega < 1$, assuming also that (H8) holds, the system has at most two steady states of the form SS4.

TABLE 1
Steady states of (1.1). All functions are defined in [Table 10](#).

	s_0, s_1, s_2 and x_0, x_1, x_2 components
SS1	$s_0 = s_0^{\text{in}}, s_1 = s_1^{\text{in}}, s_2 = s_2^{\text{in}}$ and $x_0 = 0, x_1 = 0, x_2 = 0$
SS2	$s_0 = s_0^{\text{in}}, s_1 = s_1^{\text{in}}, s_2 = M_2(D + a_2)$ and $x_0 = 0, x_1 = 0, x_2 = \frac{D}{D+a_2}(s_2^{\text{in}} - s_2)$
SS3	$s_1 = s_1^{\text{in}} + s_0^{\text{in}} - s_0$ and $s_2 = s_2^{\text{in}} - \omega(s_0^{\text{in}} - s_0)$, where s_0 is a solution of $\psi_0(s_0) = D + a_0$ and $x_0 = \frac{D}{D+a_0}(s_0^{\text{in}} - s_0), x_1 = 0, x_2 = 0$
SS4	$s_0 = M_0(D + a_0, s_2)$ and $s_1 = M_1(D + a_1, s_2)$, where s_2 is a solution of $\Psi(s_2, D) = (1 - \omega)s_0^{\text{in}} + s_1^{\text{in}} + s_2^{\text{in}}$ and $x_0 = \frac{D}{D+a_0}(s_0^{\text{in}} - s_0), x_1 = \frac{D}{D+a_1}(s_0^{\text{in}} - s_0 + s_1^{\text{in}} - s_1), x_2 = 0$
SS5	$s_0 = \varphi_0(D), s_1 = s_1^{\text{in}} + s_0^{\text{in}} - s_0, s_2 = M_2(D + a_2)$ and $x_0 = \frac{D}{D+a_0}(s_0^{\text{in}} - s_0), x_1 = 0, x_2 = \frac{D}{D+a_2}(s_2^{\text{in}} - s_2 - \omega(s_0^{\text{in}} - s_0))$
SS6	$s_0 = \varphi_0(D), s_1 = \varphi_1(D), s_2 = M_2(D + a_2)$ and $x_0 = \frac{D}{D+a_0}(s_0^{\text{in}} - s_0), x_1 = \frac{D}{D+a_1}(s_0^{\text{in}} - s_0 + s_1^{\text{in}} - s_1), x_2 = \frac{D}{D+a_2}((1 - \omega)(s_0^{\text{in}} - s_0) + s_1^{\text{in}} - s_1 + s_2^{\text{in}} - s_2)$
SS7	$s_0 = s_0^{\text{in}}$ and $s_2 = s_2^{\text{in}} + s_1^{\text{in}} - s_1$, where s_1 is a solution of $\psi_1(s_1) = D + a_1$ and $x_0 = 0, x_1 = \frac{D}{D+a_1}(s_1^{\text{in}} - s_1), x_2 = 0$
SS8	$s_0 = s_0^{\text{in}}, s_1 = \varphi_1(D), s_2 = M_2(D + a_2)$ and $x_0 = 0, x_1 = \frac{D}{D+a_1}(s_1^{\text{in}} - s_1), x_2 = \frac{D}{D+a_2}(s_1^{\text{in}} - s_1 + s_2^{\text{in}} - s_2)$

TABLE 2
Existence conditions of steady states of (1.1). All functions are given in [Table 10](#).

	Existence conditions
SS1	Always exists
SS2	$\mu_2(s_2^{\text{in}}) > D + a_2$
SS3	$\mu_0(s_0^{\text{in}}, s_2^{\text{in}}) > D + a_0$
SS4	$(1 - \omega)s_0^{\text{in}} + s_1^{\text{in}} + s_2^{\text{in}} \geq \phi_1(D), s_0^{\text{in}} > M_0(D + a_0, s_2),$ $s_0^{\text{in}} + s_1^{\text{in}} > M_0(D + a_0, s_2) + M_1(D + a_1, s_2)$ with s_2 solution of equation $\Psi(s_2, D) = (1 - \omega)s_0^{\text{in}} + s_1^{\text{in}} + s_2^{\text{in}}$
SS5	$s_0^{\text{in}} > \varphi_0(D), s_2^{\text{in}} - \omega s_0^{\text{in}} > M_2(D + a_2) - \omega \varphi_0(D)$
SS6	$(1 - \omega)s_0^{\text{in}} + s_1^{\text{in}} + s_2^{\text{in}} > \phi_2(D), s_0^{\text{in}} > \varphi_0(D), s_0^{\text{in}} + s_1^{\text{in}} > \varphi_0(D) + \varphi_1(D)$
SS7	$\mu_1(s_1^{\text{in}}, s_2^{\text{in}}) > D + a_1$
SS8	$s_1^{\text{in}} > \varphi_1(D), s_1^{\text{in}} + s_2^{\text{in}} > \varphi_1(D) + M_2(D + a_2)$

3. Stability of steady states. In this section, the necessary and sufficient conditions of stability of all steady states are given in [Table 5](#). Any reference to steady state stability should be considered as local exponential stability, that is to say, the real parts of the eigenvalues of the Jacobian matrix are negative. We need the following notations:

$$(3.1) \quad E = \frac{\partial \mu_0}{\partial s_0}(s_0, s_2), \quad F = \frac{\partial \mu_0}{\partial s_2}(s_0, s_2), \quad G = \frac{\partial \mu_1}{\partial s_1}(s_1, s_2), \quad H = -\frac{\partial \mu_1}{\partial s_2}(s_1, s_2),$$

$$(3.2) \quad I = \mu_2'(s_2), \quad J = \mu_0(s_0, s_2), \quad K = \mu_1(s_1, s_2), \quad L = \mu_2(s_2).$$

We have used the opposite sign of the partial derivative $H = -\partial \mu_1 / \partial s_2$, such that all constants involved in the computation become positive. Using the Liénard-Chipart

stability criteria, the asymptotic stability of SS4 and SS6 requires definitions and notations that are given in [Tables 3](#) and [4](#), respectively.

TABLE 3

Liénard-Chipart coefficients for SS4. The functions E, F, G, H, I, J, K and L , defined by (3.1) and (3.2), are evaluated at the components of SS4 given in [Table 1](#).

$$\begin{aligned} c_1 &= 2D + (E + \omega F)x_0 + (G + H)x_1 \\ c_2 &= D^2 + (E + \omega F)(D + J)x_0 + (G + H)(D + K)x_1 + (E(G + H) - (1 - \omega)FG)x_0x_1 \\ c_3 &= D(E + \omega F)Jx_0 + D(G + H)Kx_1 + (E(G + H) - (1 - \omega)FG)(J + K)x_0x_1 \\ c_4 &= (E(G + H) - (1 - \omega)FG)JKx_0x_1 \\ \hline \phi_4(D, s_0^{\text{in}}, s_1^{\text{in}}, s_2^{\text{in}}) &= c_1c_2c_3 - c_1^2c_4 - c_3^2 \end{aligned}$$

TABLE 4

Liénard-Chipart coefficients for SS6. The functions E, F, G, H, I, J, K and L , defined by (3.1) and (3.2), are evaluated at the components of SS6 given in [Table 1](#).

$$\begin{aligned} c_1 &= 3D + (E + Fw)x_0 + (G + H)x_1 + Ix_2 \\ c_2 &= 3D^2 + (2D + J)(E + \omega F)x_0 + (2D + K)(G + H)x_1 + EIx_0x_2 + GIx_1x_2 \\ &\quad + (2D + L)Ix_2 + (E(G + H) - (1 - \omega)FG)x_0x_1 \\ c_3 &= D^3 + D(D + 2J)(E + \omega F)x_0 + D(D + 2K)(G + H)x_1 + D(D + 2L)Ix_2 \\ &\quad + EI(D + J + L)x_0x_2 + GI(D + K + L)x_1x_2 + EGIx_0x_1x_2 + (E(G + H) \\ &\quad - (1 - \omega)FG)(D + J + K)x_0x_1 \\ c_4 &= D^2(E + \omega F)Jx_0 + D^2(G + H)Kx_1 + D^2ILx_2 + EI(DJ + DL + JL)x_0x_2 \\ &\quad + GI(DK + DL + KL)x_1x_2 + EGI(J + K + L)x_0x_1x_2 + (E(G + H) \\ &\quad - (1 - \omega)FG)(DJ + DK + JK)x_0x_1 \\ c_5 &= DEIJLx_0x_2 + DGIKLx_1x_2 + D(E(G + H) - (1 - \omega)FG)JKx_0x_1 \\ &\quad + EGI(JK + JL + KL)x_0x_1x_2 \\ c_6 &= EGIJKLx_0x_1x_2 \\ \hline r_0 &= c_1c_2 - c_3, \quad r_1 = c_1c_4 - c_5, \quad r_2 = c_3r_0 - c_1r_1, \quad r_3 = c_5r_0 - c_1^2c_6 \\ r_4 &= r_1r_2 - r_0r_3, \quad r_5 = r_3r_4 - c_1c_6r_2^2 \end{aligned}$$

Now, we can state our main result.

Theorem 3.1. Assume that Hypotheses (H1) to (H8) hold. The necessary and sufficient conditions of local stability of the steady states are given in [Table 5](#).

TABLE 5

Stability conditions of steady states of (1.1). The function ϕ_4 is given in [Table 3](#), while c_3, c_5, r_4 and r_5 are defined in [Table 4](#). All other functions are given in [Table 10](#).

Stability conditions	
SS1	$\mu_0(s_0^{\text{in}}, s_2^{\text{in}}) < D + a_0, \mu_1(s_1^{\text{in}}, s_2^{\text{in}}) < D + a_1, \mu_2(s_2^{\text{in}}) < D + a_2$
SS2	$s_0^{\text{in}} < \varphi_0(D), s_1^{\text{in}} < \varphi_1(D)$
SS3	$\mu_1(s_0^{\text{in}} + s_1^{\text{in}} - s_0, s_2^{\text{in}} - \omega(s_0^{\text{in}} - s_0)) < D + a_1, s_2^{\text{in}} - \omega s_0^{\text{in}} < M_2(D + a_2) - \omega\varphi_0(D)$ with s_0 solution of equation $\psi_0(s_0) = D + a_0$
SS4	$(1 - \omega)s_0^{\text{in}} + s_1^{\text{in}} + s_2^{\text{in}} < \phi_2(D), \phi_3(D) > 0, \frac{\partial \Psi}{\partial s_2}(s_2, D) > 0, \phi_4(D, s_0^{\text{in}}, s_1^{\text{in}}, s_2^{\text{in}}) > 0$
SS5	$s_0^{\text{in}} + s_1^{\text{in}} < \varphi_0(D) + \varphi_1(D)$
SS6	$c_3 > 0, c_5 > 0, r_4 > 0, r_5 > 0$
SS7	$s_1^{\text{in}} + s_2^{\text{in}} < M_3(s_0^{\text{in}}, D + a_0) + M_1(D + a_1, M_3(s_0^{\text{in}}, D + a_0)),$ $s_1^{\text{in}} + s_2^{\text{in}} < M_2(D + a_2) + \varphi_1(D)$
SS8	$s_0^{\text{in}} < \varphi_0(D)$

Remark 3.2. Using Lemma 3 in [\[15\]](#), we have the following results:

- If $\omega \geq 1$, the stability condition of SS4 $\frac{\partial \Psi}{\partial s_2}(s_2, D) > 0$ is always satisfied.
- If $\omega < 1$, and if $(1-\omega)s_0^{\text{in}} + s_1^{\text{in}} + s_2^{\text{in}} > \phi_1(D)$, the equation defining s_2 in [Table 1](#) has two solutions $s_2^{*1} < s_2^{*2}$, such that $\frac{\partial \Psi}{\partial s_2}(s_2^{*1}, D) < 0$ and $\frac{\partial \Psi}{\partial s_2}(s_2^{*2}, D) > 0$. We denote by SS4¹ the steady state of type SS4 corresponding to s_2^{*1} while SS4² corresponds to s_2^{*2} . When it exists, SS4¹ is unstable. When SS4² exists, its stability condition $\frac{\partial \Psi}{\partial s_2}(s_2, D) > 0$ is always satisfied.

From [Tables 2](#) and [5](#), we can deduce the following result.

Proposition 3.3.

- If SS2 or SS3 or SS7 exists then, SS1 is unstable.
- If SS6 exists then, SS2, SS4, SS5 and SS8 are unstable, when they exist.
- If SS5 exists then, SS2, SS3 and SS8 are unstable, when they exist.
- If SS8 exists then, SS7 is unstable, when it exists.

4. Applications to a three-tiered microbial 'food web'. In this section, we consider the model of a chlorophenol-mineralising three-tiered microbial 'food web' in a chemostat as application of our mathematical analysis, in order to compare our findings to the numerical results in [\[24\]](#). This model is described by the following system of differential equations

$$(4.1) \quad \begin{cases} \dot{X}_{\text{ch}} = (Y_{\text{ch}}f_0(S_{\text{ch}}, S_{\text{H}_2}) - D - k_{\text{dec, ch}})X_{\text{ch}} \\ \dot{X}_{\text{ph}} = (Y_{\text{ph}}f_1(S_{\text{ph}}, S_{\text{H}_2}) - D - k_{\text{dec, ph}})X_{\text{ph}} \\ \dot{X}_{\text{H}_2} = (Y_{\text{H}_2}f_2(S_{\text{H}_2}) - D - k_{\text{dec, H}_2})X_{\text{H}_2} \\ \dot{S}_{\text{ch}} = D(S_{\text{ch}}^{\text{in}} - S_{\text{ch}}) - f_0(S_{\text{ch}}, S_{\text{H}_2})X_{\text{ch}} \\ \dot{S}_{\text{ph}} = D(S_{\text{ph}}^{\text{in}} - S_{\text{ph}}) + \frac{224}{208}(1 - Y_{\text{ch}})f_0(S_{\text{ch}}, S_{\text{H}_2})X_{\text{ch}} - f_1(S_{\text{ph}}, S_{\text{H}_2})X_{\text{ph}} \\ \dot{S}_{\text{H}_2} = D(S_{\text{H}_2}^{\text{in}} - S_{\text{H}_2}) - \frac{16}{208}f_0(S_{\text{ch}}, S_{\text{H}_2})X_{\text{ch}} + \frac{32}{224}(1 - Y_{\text{ph}})f_1(S_{\text{ph}}, S_{\text{H}_2})X_{\text{ph}} \\ \quad - f_2(S_{\text{H}_2})X_{\text{H}_2}, \end{cases}$$

where S_{ch} , S_{ph} and S_{H_2} , are the chlorophenol, phenol and hydrogen substrates concentrations; X_{ch} , X_{ph} and X_{H_2} are the chlorophenol, phenol and hydrogen degrader concentrations; $S_{\text{ch}}^{\text{in}}$, $S_{\text{ph}}^{\text{in}}$ and $S_{\text{H}_2}^{\text{in}}$ are the input concentrations; $k_{\text{dec, ch}}$, $k_{\text{dec, ph}}$ and $k_{\text{dec, H}_2}$ are the decay rates; Y_{ch} , Y_{ph} and Y_{H_2} are the yield coefficients, respectively; $224/208(1 - Y_{\text{ch}})$ represents the fraction of chlorophenol converted to phenol; $32/224(1 - Y_{\text{ph}})$ represents the fraction of phenol that is transformed to hydrogen and $16/208$ represents the fraction of hydrogen consumed by the chlorophenol degrader. The specific growth rates take the form:

$$(4.2) \quad \begin{aligned} f_0(S_{\text{ch}}, S_{\text{H}_2}) &= \frac{k_{m, \text{ch}} S_{\text{ch}}}{K_{S, \text{ch}} + S_{\text{ch}}} \frac{S_{\text{H}_2}}{K_{S, \text{H}_2, c} + S_{\text{H}_2}}, \\ f_1(S_{\text{ph}}, S_{\text{H}_2}) &= \frac{k_{m, \text{ph}} S_{\text{ph}}}{K_{S, \text{ph}} + S_{\text{ph}}} \frac{1}{1 + S_{\text{H}_2}/K_{I, \text{H}_2}}, \quad f_2(S_{\text{H}_2}) = \frac{k_{m, \text{H}_2} S_{\text{H}_2}}{K_{S, \text{H}_2} + S_{\text{H}_2}}, \end{aligned}$$

The biological parameter values, used in [\[24\]](#), are provided in [Table 14](#). Following [\[19\]](#), the rescaling of the variables [\(E.1\)](#) and [\(E.2\)](#) can reduce [\(4.1\)](#) to the form [\(1.1\)](#), that is, the yields coefficients in [\(4.1\)](#) are normalized to one, except one of them which is equal to $\omega \simeq 0.53$. Under this rescaling [\(E.1\)](#) and [\(E.2\)](#), the growth functions [\(4.2\)](#) take the form [\(E.3\)](#) keeping their form of a double Monod, a Monod with product inhibition, and a Monod kinetics, respectively, so that Hypotheses (H1) to (H8) are satisfied. Therefore, [Theorem 2.1](#) and [Theorem 3.1](#), with $\omega < 1$, apply and give rigorous proofs for the results of [\[24\]](#), on existence and stability of steady states, which, for the most part, have only been obtained numerically. See [Appendix E](#) for the details.

In the following, we consider $S_{\text{ph}}^{\text{in}} = 0$ and $S_{\text{H}_2}^{\text{in}} = 2.67 \times 10^{-5}$, corresponding to Fig. 3(a) in [24] and we fix $D = 0.01$ and we determine the bifurcation diagram, where the input concentration $S_{\text{ch}}^{\text{in}}$ is the bifurcation parameter. This choice for the operating parameters is identical to that in [15] excepted that we have added the microbial decay terms, as in [24]. Our aim is to compare our results to those of [24] and to see if there are interesting phenomena that were not detected in the operating diagram depicted in Fig. 3(a) of [24], see Remark 4.2 below. Our aim is also to see the effects of mortality on the behavior of the process and to compare our bifurcation diagram to the one depicted in [15], see Remark 4.3 below. Using Theorem 2.1 and Theorem 3.1, we have the following result.

Proposition 4.1. Let $S_{\text{ph}}^{\text{in}} = 0$, $S_{\text{H}_2}^{\text{in}} = 2.67 \times 10^{-5}$ and $D = 0.01$. Notice that in this case SS7 and SS8 do not exist. Using the biological parameter values in Table 14, the bifurcation values σ_i , $i = 1, \dots, 6$ are provided in Table 6. The bifurcation analysis of (4.1) according to $S_{\text{ch}}^{\text{in}}$ is given in Table 7. The bifurcation types at the critical values σ_i are defined in Table 8.

TABLE 6

Critical parameter values σ_i , for $i = 1, \dots, 6$ where Y is defined in Appendix E, r_5 in Table 4 while all other functions are given in Table 10. Note that $\sigma_1 < \sigma_3 < \sigma_4 < \sigma_2 < \sigma_5 < \sigma_6$, compare with Table 5 in [15].

Definition	Value
$\sigma_1 = M_0 (D + a_0, S_{\text{H}_2}^{\text{in}}) / Y$	0.003173
$\sigma_2 = (\phi_1(D) - S_{\text{H}_2}^{\text{in}}) / ((1 - \omega)Y)$	0.029402
$\sigma_3 = \varphi_0(D) / Y$	0.013643
$\sigma_4 = (S_{\text{H}_2}^{\text{in}} - M_2(D + a_2) + \omega\varphi_0(D)) / (\omega Y)$	0.013985
$\sigma_5 = (\phi_2(D) - S_{\text{H}_2}^{\text{in}}) / ((1 - \omega)Y)$	0.033292
σ_6 is the largest root of equation $r_5 = 0$	0.1025

TABLE 7

Existence and stability of steady states, with respect to $S_{\text{ch}}^{\text{in}}$. The bifurcation values σ_i , $i = 1, \dots, 6$ are given in Table 6. The letter S (resp. U) means that the corresponding steady state is stable (resp. unstable). No letter means that the steady state does not exist.

Interval	SS1	SS2	SS3	SS4 ¹	SS4 ²	SS5	SS6
$0 < S_{\text{ch}}^{\text{in}} < \sigma_1$	U	S					
$\sigma_1 < S_{\text{ch}}^{\text{in}} < \sigma_3$	U	S	U				
$\sigma_3 < S_{\text{ch}}^{\text{in}} < \sigma_4$	U	U	U			S	
$\sigma_4 < S_{\text{ch}}^{\text{in}} < \sigma_2$	U	U	S				
$\sigma_2 < S_{\text{ch}}^{\text{in}} < \sigma_5$	U	U	S	U	U		
$\sigma_5 < S_{\text{ch}}^{\text{in}} < \sigma_6$	U	U	S	U	U		U
$\sigma_6 < S_{\text{ch}}^{\text{in}}$	U	U	S	U	U		S

Proof. This is supported by numerical experimentation and is given in Appendix C. \square

Remark 4.2. Not all of the behaviors described in Table 7 were reported in [24]. For $D = 0.01$, the operating diagram of Fig. 3(a) in [24] predicts only three possible behaviors: the stability of SS2, the stability of SS3 and the bistability between SS3 and SS6. Note that the destabilization of SS6 via a Hopf bifurcation with emergence of a stable limit cycle has not been observed in [24]. Even, the possibility of stability of SS5 has not been reported in the operating diagram. Indeed, Fig. 3(a) of [24] does not correctly describe the transition from the region labeled SS2 (and corresponding

TABLE 8

Bifurcation types corresponding to the critical values of σ_i , $i = 1, \dots, 6$, defined in Table 6. There exists also a critical value $\sigma^* \simeq 0.099295 \in (\sigma_5, \sigma_6)$ corresponding to the value of $S_{\text{ch}}^{\text{in}}$ where the stable limit cycle disappears when $S_{\text{ch}}^{\text{in}}$ is decreasing.

Bifurcation types	
σ_1	Transcritical bifurcation of SS1 and SS3
σ_2	Saddle-node bifurcation of SS4 ¹ and SS4 ²
σ_3	Transcritical bifurcation of SS2 and SS5
σ_4	Transcritical bifurcation of SS3 and SS5
σ_5	Transcritical bifurcation of SS4 ¹ and SS6
σ_6	Supercritical Hopf bifurcation
σ^*	Disappearance of the stable limit cycle

to the stability of SS2) to the SS3 region. Our results show that this transition is via a SS5 region. The existence of the SS5 region was depicted in Fig. 3(b) of [24] in the case where $S_{\text{H}_2}^{\text{in}} = 2.67 \times 10^{-2}$. However, this region also exists when $S_{\text{H}_2}^{\text{in}} = 2.67 \times 10^{-5}$, but it is very thin, since for $D = 0.01$ it corresponds to $\sigma_3 < S_{\text{ch}}^{\text{in}} < \sigma_4$, where $\sigma_3 \simeq 0.013643$ and $\sigma_4 \simeq 0.013985$.

Figures 4.1 and 4.2 show the one-parameter bifurcation diagrams of X_{ch} and X_{H_2} versus $S_{\text{ch}}^{\text{in}}$ in system (4.1), respectively. The magnifications of the bifurcation diagrams are illustrated in Figure 4.1(b), Figure 4.2(b) and Figure 4.3 showing the transcritical bifurcations at σ_1 , σ_3 , σ_4 and σ_5 , the saddle-node bifurcation at σ_2 , the Hopf bifurcation at σ_6 and the disappearance of the cycle at σ^* . In Figure 4.1(b), SS1 and SS2 cannot be distinguished since they have both a zero X_{ch} -component. As SS2 is stable and SS1 is unstable for $S_{\text{ch}}^{\text{in}} < \sigma_3$, the $X_{\text{ch}} = 0$ axis is plotted in blue as the color of SS2 in Table 9. In Figure 4.2(b), SS1 and SS2 are distinguished but it is not the case for SS1 and SS3, since they have both a zero X_{H_2} -component. As SS3 is stable and SS1 is unstable for $S_{\text{ch}}^{\text{in}} > \sigma_4$, the $X_{\text{H}_2} = 0$ axis is plotted in purple as the color of SS3 in Table 9.

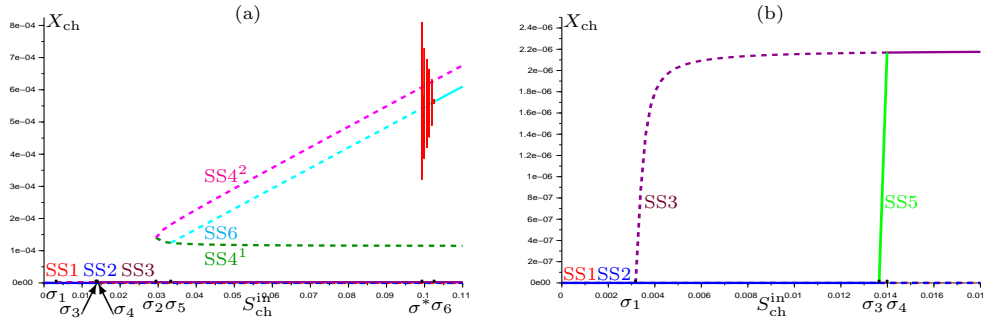


FIG. 4.1. (a) Bifurcation diagram of X_{ch} versus $S_{\text{ch}}^{\text{in}} \in [0, 0.11]$ in model (4.1) showing the appearance and disappearance of stable limit cycles. (b) Magnification on the transcritical bifurcations for $S_{\text{ch}}^{\text{in}} \in [0, 0.018]$.

TABLE 9

Colors used in Figures 4.1 to 4.3. The solid (resp. dashed) lines are used for stable (resp. unstable) steady states.

SS1	SS2	SS3	SS4 ¹	SS4 ²	SS5	SS6
Red	Blue	Purple	Dark Green	Magenta	Green	Cyan

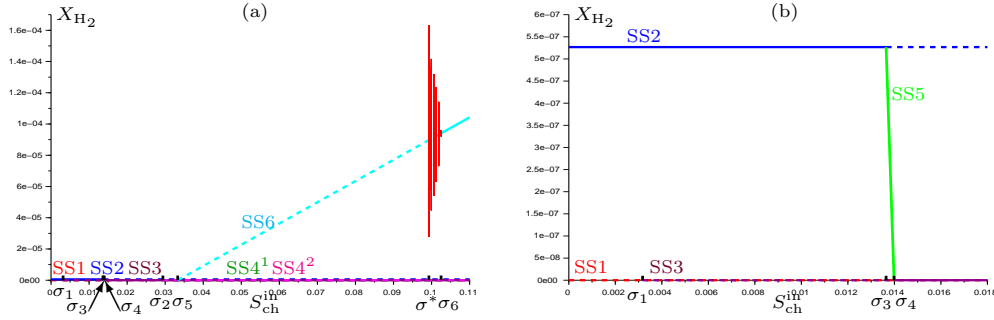


FIG. 4.2. (a) Bifurcation diagram of X_{H_2} versus $S_{ch}^{in} \in [0, 0.11]$ in model (4.1). (b) Magnification on the transcritical bifurcations for $S_{ch}^{in} \in [0, 0.018]$.

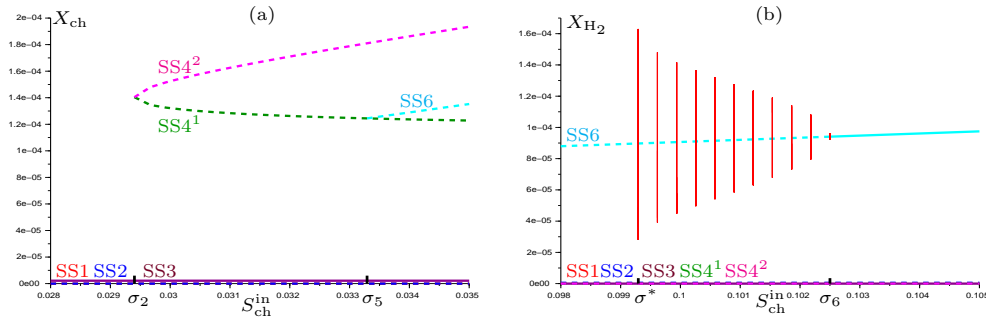


FIG. 4.3. (a) Magnification on the saddle-node bifurcation at $S_{ch}^{in} = \sigma_2$ and the transcritical bifurcation at $S_{ch}^{in} = \sigma_5$ for $S_{ch}^{in} \in [0.028, 0.035]$. (b) Magnification on the limit cycles for $S_{ch}^{in} \in [0.098, 0.105]$.

Remark 4.3. Note that the change in all bifurcation values σ_i , $i = 1, \dots, 6$ compared to [15] is predictable since their formulas in Table 6 involve the added decay terms. However, the saddle-node bifurcation at σ_2 arises after and not before the transcritical bifurcations at σ_3 and σ_4 as in [15].

We present in Figures 4.4 to 4.6 (and also Figures F.1 to F.4), the numerical simulations which illustrate our findings. We illustrate, in particular, the interesting three cases where the steady states SS1, SS2, SS4¹ and SS4² are unstable:

- For $S_{ch}^{in} \in (\sigma_5, \sigma^*)$, the numerical simulations done for various positive initial conditions permit to conjecture the global asymptotic stability of SS3 (see Figure 4.4).
- For $S_{ch}^{in} \in (\sigma^*, \sigma_6)$, the system exhibits a bistability with two basins of attraction: one toward the stable limit cycle and the second toward SS3. Figure 4.5 illustrates that the trajectories in pink and blue converge toward the stable limit cycle in red, while the green trajectory converges toward SS3. For the initial condition in Table 13, the time course in Figure F.1 illustrates the positive, periodic solution representing the coexistence of the three species. The sustained oscillations prove the stability of the limit cycle. However, Figure F.2 shows the time course of the green trajectory in Figure 4.5.
- For $S_{ch}^{in} > \sigma_6$, the system exhibits a bistability between SS6 and SS3. Figure 4.6 shows that the blue trajectory converges to the stable focus SS6, while the green trajectory converges to SS3. Figures F.3 and F.4 illustrate the time courses corresponding to the blue and the green trajectories in Figure 4.6, respectively.

Numerical simulations have shown that the stable limit cycle disappears at the

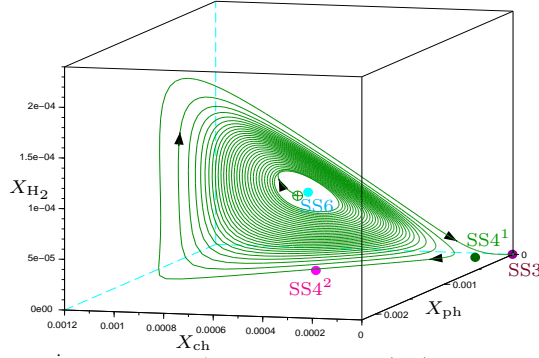


FIG. 4.4. Case $S_{ch}^{in} = 0.098 < \sigma^*$: the solution of (4.1) converges to $SS3$.

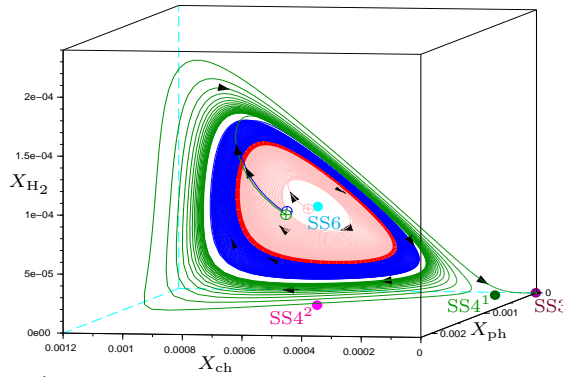


FIG. 4.5. Case $\sigma^* < S_{ch}^{in} = 0.0995 < \sigma_6$: bistability with convergence either to the stable limit cycle (in red) or to $SS3$.

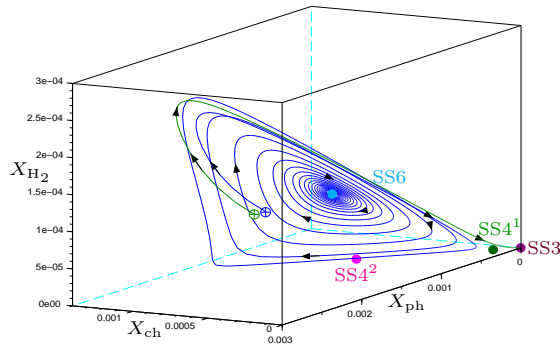


FIG. 4.6. Case $\sigma_6 < S_{ch}^{in} = 0.11$: bistability with convergence either to $SS6$ or to $SS3$.

critical value $\sigma^* \in (\sigma_5, \sigma_6)$ as S_{ch}^{in} decreases. Similarly to the numerical study of the bifurcation diagram with respect to the parameter D in [22] in the case without maintenance and $s_1^{in} = s_2^{in} = 0$, we conjecture that in our case also the stable limit cycle disappears through a saddle-node bifurcation with another unstable limit cycle when S_{ch}^{in} decreases.

5. Conclusion. In this study, we discussed the dynamics of three interacting microbial species describing a chlorophenol-mineralising three-tiered ‘food web’ in the

chemostat (4.1), introduced by Wade et al. [24]. In [24], following previous work [27] on a two-tiered model, this three-tiered microbial ‘food web’, was proposed as a reduced model of the widely used ADM1. In [24], the existence and stability of the steady states of model (4.1) have been analyzed as a function of the operating parameters (input substrate concentrations and dilution rate), using numerical tools and specific values of the biological parameters.

In this paper, we gave a complete analysis of the dynamics of the model (1.1) which generalizes (4.1) by allowing a larger class of growth functions. The existence of the steady states was analytically characterized in [15] where it was shown that model (1.1) can have up to eight types of steady states: the washout steady state denoted by SS1, six types of boundary steady states where one or two degrader populations are extinct denoted by SS2, SS3, SS4, SS5, SS7 and SS8, and a positive steady state, denoted by SS6, where all microbial populations coexist. When they exist, all steady states are unique, except the steady state SS4 where chlorophenol and phenol degraders are maintained and the hydrogen degrader is eliminated. Here we focus on the stability of steady states. We have managed to characterize the stability in this six-dimensional system, although it is generally accepted that the Routh–Hurwitz theorem is intractable beyond five dimensions. For this, we have used the Liénard–Chipart stability criteria. For SS1, SS2, SS3 and SS7, the stability conditions are determined explicitly. For SS5 and SS8, we explicitly characterize the stability conditions using the Liénard–Chipart criteria. For SS4 and SS6, the stability is given with respect to the signs of the Liénard–Chipart coefficients, defined in Tables 3 and 4. We use numerical experimentation (see Appendix C) to plot the functions, whose signs cannot be determined analytically. As shown in Appendix E, our presentation of the existence and stability issue fully clarifies the numerical study made in [24] on the three-tiered ‘food web’ model (4.1).

Our work extends all results on the stability of the existing literature [7, 15, 19, 22], which were obtained only in the case without maintenance, where the six-dimensional system (1.1) can be reduced to a three-dimensional one. We show that for SS4, which can exist in two forms, at most one steady state can be stable, a fact that was already noticed (when maintenance is not included in the model) in the particular case without phenol and hydrogen input concentrations, studied in [19] and in the general case, where these input concentrations are added, studied in [15].

We highlighted several possible asymptotic behaviors in this six-dimensional system, including the stability of the positive steady state and a boundary steady state, or the stability of a positive limit cycle and a boundary steady state, so that the long term behavior depends on the initial condition. We proved that the positive steady state of coexistence of all species can be unstable and we give numerical evidence for the supercritical Hopf bifurcation, in the case including chlorophenol and hydrogen input concentrations. The possibility of the Hopf bifurcation of the positive steady state was previously observed in [19] in the case without phenol and hydrogen input concentrations. It was analytically proved in [22], in the case without maintenance.

In order to gain more insight into the behavior of the system, we give a bifurcation diagram with the chlorophenol input concentration as the bifurcating parameter (see Figures 4.4 to 4.6) showing that one of the operating diagrams obtained numerically in [24] has omitted important transition phenomena between steady states. If the chlorophenol input concentration is too low, both the chlorophenol and phenol degraders are eliminated from the reactor and only the hydrogen degrader is maintained (SS2 is the only stable steady state). Increasing the input chlorophenol concentration, only the chlorophenol and hydrogen degraders are maintained (SS5 is the only stable

steady state). Increasing further, only the chlorophenol degrader is maintained (SS3 is the only stable steady state). For higher chlorophenol input concentration, the system exhibits a bistability behavior where either only the chlorophenol degrader is maintained (SS3 is stable) or the coexistence of three microbial species may occur around periodic oscillations (SS6 is unstable and a stable limit cycle exists). Finally, for high chlorophenol input concentration, the system exhibits a bistability behavior where either only the chlorophenol degrader is maintained or the coexistence of three microbial species occurs at a positive steady state (SS3 and SS6 are both stable).

For making our theoretical results useful in practice, one should have a description of the operating diagrams, giving the existence and stability of steady states regions with respect to the operating parameters. In a future work, we will use our results to determine analytically the operating diagrams by studying the effect of mortality on the stability regions and the coexistence of species in a three-tiered microbial 'food web'.

Appendix A. Auxiliary functions. For the description of the steady states given in [Table 1](#), together with the statement of their conditions of existence and stability, we need to define some auxiliary functions that are listed in [Table 10](#). Using Hypotheses (H1) to (H7), the existence and definition domains of these functions are all relatively straightforward and can be found as in [\[19\]](#).

TABLE 10
Notations, intervals and auxiliary functions.

Definition	
$s_i = M_i(y, s_2)$ $i = 0, 1$	Let $s_2 \geq 0$. $s_i = M_i(y, s_2)$ is the unique solution of $\mu_i(s_i, s_2) = y$, for all $0 \leq y < \mu_i(+\infty, s_2)$
$s_2 = M_2(y)$	$s_2 = M_2(y)$ is the unique solution of $\mu_2(s_2) = y$, for all $0 \leq y < \mu_2(+\infty)$
$s_2 = M_3(s_0, z)$	Let $s_0 \geq 0$. $s_2 = M_3(s_0, z)$ is the unique solution of $\mu_0(s_0, s_2) = z$, for all $0 \leq z < \mu_0(s_0, +\infty)$
$s_2^i = s_2^i(D)$ $i = 0, 1$	$s_2^i = s_2^i(D)$ is the unique solution of $\mu_i(+\infty, s_2) = D + a_i$, for all $D + a_0 < \mu_0(+\infty, +\infty)$, $\mu_1(+\infty, +\infty) < D + a_1 < \mu_1(+\infty, 0)$, resp.
I_1, I_2	$I_1 = \{D \geq 0 : s_2^0 < s_2^1\}$, $I_2 = \{D \in I_1 : s_2^0 < M_2(D + a_2) < s_2^1\}$
$\Psi(s_2, D)$	$\Psi(s_2, D) = (1 - \omega)M_0(D + a_0, s_2) + M_1(D + a_1, s_2) + s_2$, for all $D \in I_1$ and $s_2^0 < s_2 < s_2^1$
$\phi_1(D)$	$\phi_1(D) = \inf_{s_2^0 < s_2 < s_2^1} \Psi(s_2, D)$, for all $D \in I_1$
$\phi_2(D)$	$\phi_2(D) = \Psi(M_2(D + a_2), D)$, for all $D \in I_2$
$\phi_3(D)$	$\phi_3(D) = \frac{\partial \Psi}{\partial s_2}(M_2(D + a_2), D)$, for all $D \in I_2$
J_0, J_1	$J_0 = (\max(0, s_0^{\text{in}} - s_2^{\text{in}}/\omega), s_0^{\text{in}})$, $J_1 = (0, s_1^{\text{in}})$
$\psi_0(s_0)$	$\psi_0(s_0) = \mu_0(s_0, s_2^{\text{in}} - \omega(s_0^{\text{in}} - s_0))$, for all $s_0 \geq \max(0, s_0^{\text{in}} - s_2^{\text{in}}/\omega)$
$\psi_1(s_1)$	$\psi_1(s_1) = \mu_1(s_1, s_2^{\text{in}} + s_1^{\text{in}} - s_1)$, for all $s_1 \in [0, s_1^{\text{in}} + s_2^{\text{in}}]$
$\varphi_i(D)$ $i = 0, 1$	$\varphi_i(D) = M_i(D + a_i, M_2(D + a_2))$, resp., for all, $D \in \{D \geq 0 : s_2^0 < M_2(D + a_2)\}$, $D \in \{D \geq 0 : M_2(D + a_2) < s_2^1\}$

Appendix B. Proofs.

B.1. Proof of [Theorem 3.1](#). The local stability of the steady states is determined by the eigenvalues of the Jacobian matrix of system [\(1.1\)](#) evaluated at the

steady state. The Jacobian matrix of (1.1) corresponds to the 6×6 matrix:

$$\mathcal{J} = \begin{bmatrix} J-D-a_0 & 0 & 0 & Ex_0 & 0 & Fx_0 \\ 0 & K-D-a_1 & 0 & 0 & Gx_1 & -Hx_1 \\ 0 & 0 & L-D-a_2 & 0 & 0 & Ix_2 \\ -J & 0 & 0 & -D-Ex_0 & 0 & -Fx_0 \\ J & -K & 0 & Ex_0 & -D-Gx_1 & Fx_0+Hx_1 \\ -\omega J & K & -L & -\omega Ex_0 & Gx_1 & -D-\omega Fx_0-Hx_1-Ix_2 \end{bmatrix},$$

where the functions E, F, G, H, I, J, K and L are defined by (3.1) and (3.2), and are evaluated at the steady state. The stability of the steady state is investigated by analyzing the real parts of the eigenvalues of \mathcal{J} , which are the roots of the characteristic polynomial.

For SS1, the characteristic polynomial is

$$P_1(\lambda) = (\lambda - \lambda_1)(\lambda - \lambda_2)(\lambda - \lambda_3)(\lambda + D)^3,$$

where $\lambda_1 = \mu_0(s_0^{\text{in}}, s_2^{\text{in}}) - D - a_0$, $\lambda_2 = \mu_1(s_1^{\text{in}}, s_2^{\text{in}}) - D - a_1$ and $\lambda_3 = \mu_2(s_2^{\text{in}}) - D - a_2$. Therefore, SS1 is stable if and only if $\lambda_1 < 0$, $\lambda_2 < 0$ and $\lambda_3 < 0$, that is, the stability conditions of SS1 in Table 5 hold.

For SS2, the characteristic polynomial is

$$P_2(\lambda) = (\lambda - \lambda_1)(\lambda - \lambda_2)(\lambda + D)^2(\lambda^2 + c_1\lambda + c_2),$$

where $\lambda_1 = \mu_0(s_0^{\text{in}}, M_2(D + a_2)) - D - a_0$, $\lambda_2 = \mu_1(s_1^{\text{in}}, M_2(D + a_2)) - D - a_1$, $c_1 = D + Ix_2$ and $c_2 = LIx_2$. Since $c_1 > 0$ and $c_2 > 0$, the real parts of the roots of the quadratic factor are negative. Therefore, SS2 is stable if and only if $\lambda_1 < 0$ and $\lambda_2 < 0$. Since M_0 and M_1 are increasing, these conditions are equivalent to the stability conditions of SS2 in Table 5.

For SS3, the characteristic polynomial is

$$P_3(\lambda) = (\lambda - \lambda_1)(\lambda - \lambda_2)(\lambda + D)^2(\lambda^2 + c_1\lambda + c_2),$$

where

$\lambda_1 = \mu_1(s_0^{\text{in}} - s_0 + s_1^{\text{in}}, s_2^{\text{in}} - \omega(s_0^{\text{in}} - s_0)) - D - a_1$, $\lambda_2 = \mu_2(s_2^{\text{in}} - \omega(s_0^{\text{in}} - s_0)) - D - a_2$, $c_1 = D + (E + \omega F)x_0$ and $c_2 = J(E + \omega F)x_0$, where s_0 is the solution in the interval J_0 of equation $\psi_0(s_0) = D + a_0$. Since $c_1 > 0$ and $c_2 > 0$, the real parts of the roots of the quadratic factor are negative. Therefore, SS3 is stable if and only if $\lambda_1 < 0$ and $\lambda_2 < 0$. The condition $\lambda_1 < 0$ is the first stability condition of SS3 in Table 5. Since M_2 is increasing, the condition $\lambda_2 < 0$ is equivalent to

$$(B.1) \quad s_2^{\text{in}} - \omega(s_0^{\text{in}} - s_0) < M_2(D + a_2) \iff s_0 < (M_2(D + a_2) - s_2^{\text{in}}) / \omega + s_0^{\text{in}}.$$

As the function ψ_0 is increasing, (B.1) is equivalent to

$$(B.2) \quad \psi_0(s_0) < \psi_0((M_2(D + a_2) - s_2^{\text{in}}) / \omega + s_0^{\text{in}}).$$

From the definition of the function ψ_0 together with the condition $\psi_0(s_0) = D + a_0$ defining s_0 , we deduce that (B.2) is equivalent to

$$D + a_0 < \mu_0((M_2(D + a_2) - s_2^{\text{in}}) / \omega + s_0^{\text{in}}, M_2(D + a_2)).$$

Since M_0 is increasing, this condition is equivalent to the second stability condition of SS3 in Table 5.

For SS4, the characteristic polynomial is

$$P_4(\lambda) = (\lambda - \lambda_1)(\lambda + D) (\lambda^4 + c_1\lambda^3 + c_2\lambda^2 + c_3\lambda + c_4),$$

where $\lambda_1 = \mu_2(s_2) - D - a_2$ with s_2 is defined in [Table 1](#) and the coefficients c_i for $i = 1, \dots, 4$ are defined in [Table 3](#). From [Lemma D.1](#), all of the roots of the fourth order polynomial have negative real parts if and only if $c_i > 0$, for $i = 1, 3, 4$ and $r_1 = c_1c_2c_3 - c_1^2c_4 - c_3^2 > 0$. From the expression of c_1 given in [Table 3](#), we always have $c_1 > 0$. Moreover, $c_3 > 0$ and $c_4 > 0$ if and only if

$$(B.3) \quad E(G + H) - (1 - \omega)FG > 0.$$

Let $s_2 > 0$. Under (H4) and (H5), we have

$$\begin{aligned} \frac{\partial M_0}{\partial s_2}(y, s_2) &= -\frac{\partial \mu_0}{\partial s_2}(M_0(y, s_2), s_2) \left[\frac{\partial \mu_0}{\partial s_0}(M_0(y, s_2), s_2) \right]^{-1}, \text{ for all } y \in (0, \mu_0(+\infty, s_2)), \\ \frac{\partial M_1}{\partial s_2}(y, s_2) &= -\frac{\partial \mu_1}{\partial s_2}(M_1(y, s_2), s_2) \left[\frac{\partial \mu_1}{\partial s_1}(M_1(y, s_2), s_2) \right]^{-1}, \text{ for all } y \in (0, \mu_1(+\infty, s_2)). \end{aligned}$$

Using [\(3.1\)](#), we obtain

$$\frac{\partial M_0}{\partial s_2}(D + a_0, s_2) = -\frac{F}{E} \quad \text{and} \quad \frac{\partial M_1}{\partial s_2}(D + a_1, s_2) = \frac{H}{G}.$$

Moreover, we have for all $s_2 \in (s_2^0, s_2^1)$ and $D \in I_1$,

$$(B.4) \quad \frac{\partial \Psi}{\partial s_2}(s_2, D) = (1 - \omega) \frac{\partial M_0}{\partial s_2}(D + a_0, s_2) + \frac{\partial M_1}{\partial s_2}(D + a_1, s_2) + 1.$$

Using [\(B.4\)](#), it follows that

$$\frac{\partial \Psi}{\partial s_2}(s_2, D) = -\frac{F}{E}(1 - \omega) + \frac{H}{G} + 1 = \frac{E(G+H) - (1-\omega)FG}{EG}.$$

Since E and G are positive, condition [\(B.3\)](#) is equivalent to $\frac{\partial \Psi}{\partial s_2}(s_2, D) > 0$.

From the definition of ϕ_4 given in [Table 3](#) and since μ_2 is increasing, it follows that, SS4 is stable if and only if

$$(B.5) \quad s_2 < M_2(D + a_2), \quad \frac{\partial \Psi}{\partial s_2}(s_2, D) > 0 \quad \text{and} \quad \phi_4(D, s_0^{\text{in}}, s_1^{\text{in}}, s_2^{\text{in}}) > 0.$$

which is equivalent to the stability condition in [Table 5](#) because this first condition of [\(B.5\)](#) is equivalent the first and the second one of SS4 in [Table 5](#) (similarly to the proof of Theorem 2 in [\[15\]](#)).

For SS5, the characteristic polynomial is

$$P_5(\lambda) = (\lambda - \lambda_1)(\lambda + D) (\lambda^4 + c_1\lambda^3 + c_2\lambda^2 + c_3\lambda + c_4),$$

where $\lambda_1 = \mu_1(s_0^{\text{in}} + s_1^{\text{in}} - M_0(D + a_0, M_2(D + a_2)), M_2(D + a_2)) - D - a_1$ and the coefficients c_i are given by:

$$\begin{aligned} c_1 &= 2D + (E + \omega F)x_0 + Ix_2, \\ c_2 &= D^2 + (E + \omega F)(D + J)x_0 + I(D + L)x_2 + EIx_0x_2, \\ c_3 &= D(E + \omega F)Jx_0 + DILx_2 + EI(J + L)x_0x_2 \quad \text{and} \quad c_4 = EIJLx_0x_2. \end{aligned}$$

From [Lemma D.1](#), the roots of the fourth order polynomial are of negative real parts if and only if

$$(B.6) \quad c_i > 0, \quad \text{for } i = 1, 3, 4 \quad \text{and} \quad r_1 = c_1c_2c_3 - c_1^2c_4 - c_3^2 > 0.$$

We always have $c_i > 0$ for $i = 1, 3, 4$. We can write r_1 as follows:

$$\begin{aligned} r_1 = & DJ [(D+J)(E+\omega F)^3 - E^3 J] x_0^3 + D^2 I^3 L x_2^3 + E^2 I^2 (E+\omega F)(J+L) x_0^3 x_2^2 + DEI^3 (J+2L) x_0 x_2^3 \\ & + E^2 I^3 (J+L) x_0^2 x_2^3 + EI [D(2J+L)(E+\omega F)^2 + \omega F J^2 (2E+\omega F)] x_0^3 x_2 + 3D^3 I^2 L x_2^2 \\ & + D^2 J [3D(E+\omega F)^2 + F\omega J(2E+\omega F)] x_0^2 + EI^2 [D(J+L)(5E+3\omega F) + F\omega (J^2+L^2)] x_0^2 x_2^2 \\ & + DI [F\omega (DF\omega(2J+L) + F\omega J(J+2L) + DE(9J+5L) + 2EJ^2) + DE^2(7J+4L)] x_0^2 x_2 \\ & + DI^2 [DE(4J+7L) + F\omega L(2J+L) + DF\omega(J+2L)] x_0 x_2^2 + 2D^4 J(E+\omega F) x_0 + 2D^4 I L x_2 \\ & + D^2 I [D(J+L)(5E+3\omega F) + 2F\omega J L] x_0 x_2 + (D^2 + DE x_0 + DI x_2 + EI x_0 x_2) (EJ x_0 - IL x_2)^2. \end{aligned}$$

Thus, $r_1 > 0$. Consequently, the conditions (B.6) are satisfied. Therefore, SS5 is stable if and only if $\lambda_1 < 0$. Since M_1 is increasing, this condition is equivalent to the stability condition of SS5 in Table 5.

For SS6, the characteristic polynomial is given by:

$$P_6(\lambda) = \lambda^6 + c_1 \lambda^5 + c_2 \lambda^4 + c_3 \lambda^3 + c_4 \lambda^2 + c_5 \lambda + c_6,$$

where c_i , $i = 1, \dots, 6$ are defined in Table 4. From Lemma D.2, all of the roots of the sixth order polynomial have negative real parts if and only if $c_i > 0$, $i = 1, 3, 5, 6$ and $r_j > 0$, $j = 4, 5$, where c_i and r_j are listed in Table 4. Since c_1 and c_6 are positive, the proof is complete.

For SS7, the characteristic polynomial is

$$P_7(\lambda) = (\lambda - \lambda_1)(\lambda - \lambda_2)(\lambda + D)^2(\lambda^2 + c_1 \lambda + c_2),$$

where $\lambda_1 = \mu_0 (s_0^{\text{in}}, s_1^{\text{in}} - s_1 + s_2^{\text{in}}) - D - a_0$, $\lambda_2 = \mu_2 (s_1^{\text{in}} - s_1 + s_2^{\text{in}}) - D - a_2$, $c_1 = D + (G+H)x_1$ and $c_2 = K(G+H)x_1$ where s_1 is the solution in the interval J_1 of equation $\psi_1(s_1) = D + a_1$. Since $c_1 > 0$ and $c_2 > 0$, the real parts of the roots of the quadratic factor are negative. Therefore, SS7 is stable if and only if $\lambda_1 < 0$ and $\lambda_2 < 0$. Since the functions M_2 and M_3 are increasing, the conditions $\lambda_1 < 0$ and $\lambda_2 < 0$ are equivalent to

$$(B.7) \quad s_1 > s_1^{\text{in}} + s_2^{\text{in}} - M_3(s_0^{\text{in}}, D + a_0) \quad \text{and} \quad s_1 > s_1^{\text{in}} + s_2^{\text{in}} - M_2(D + a_2).$$

Since the function ψ_1 is increasing, (B.7) is equivalent to

$$\psi_1(s_1) > \psi_1(s_1^{\text{in}} + s_2^{\text{in}} - M_3(s_0^{\text{in}}, D + a_0)), \quad \psi_1(s_1) > \psi_1(s_1^{\text{in}} + s_2^{\text{in}} - M_2(D + a_2)).$$

From the definition of the function ψ_1 together with the condition $\psi_1(s_1) = D + a_1$ which defines s_1 , the preceding conditions are equivalent to

$$\begin{aligned} \mu_1 (s_1^{\text{in}} + s_2^{\text{in}} - M_3(s_0^{\text{in}}, D + a_0), M_3(s_0^{\text{in}}, D + a_0)) &< D + a_1, \\ \mu_1 (s_1^{\text{in}} + s_2^{\text{in}} - M_2(D + a_2), M_2(D + a_2)) &< D + a_1. \end{aligned}$$

Since M_1 is increasing, these conditions are equivalent to the stability conditions of SS7 in Table 5.

For SS8, the characteristic polynomial is

$$P_8(\lambda) = (\lambda - \lambda_1)(\lambda + D) (\lambda^4 + c_1 \lambda^3 + c_2 \lambda^2 + c_3 \lambda + c_4),$$

where $\lambda_1 = \mu_0 (s_0^{\text{in}}, M_2(D + a_2)) - D - a_0$ and the coefficients c_i are given by:

$$\begin{aligned} c_1 &= 2D + (G+H)x_1 + Ix_2, \\ c_2 &= D^2 + (G+H)(D+K)x_1 + I(D+L)x_2 + GIx_1x_2, \\ c_3 &= D(G+H)Kx_1 + DILx_2 + GI(K+L)x_1x_2 \quad \text{and} \quad c_4 = GIKLx_1x_2. \end{aligned}$$

From [Lemma D.1](#), the roots of the fourth order polynomial are of negative real parts if and only if

$$(B.8) \quad c_i > 0, \quad \text{for } i = 1, 3, 4 \quad \text{and} \quad r_1 = c_1 c_2 c_3 - c_1^2 c_4 - c_3^2 > 0.$$

We always have $c_i > 0$, for $i = 1, 3, 4$. We can write r_1 as follows:

$$\begin{aligned} r_1 = & DK [(D+K)(G+H)^3 - G^3 K] x_1^3 + D^2 I^3 L x_2^3 + G^2 I^2 (G+H)(K+L) x_1^3 x_2^2 + G^2 I^3 (K+L) x_1^2 x_2^3 \\ & + GI [D(2K+L)(G+H)^2 + HK^2(2G+H)] x_1^3 x_2 + DGI^3 (K+2L) x_1 x_2^3 + 3D^3 I^2 L x_2^2 \\ & + D^2 K [3D(G+H)^2 + HK(2G+H)] x_1^2 + GI^2 [D(K+L)(5G+3H) + H(K^2+L^2)] x_1^2 x_2^2 \\ & + DI [H(DH(2K+L) + HK(K+2L) + DG(9K+5L) + 2GK^2) + DG^2(7K+4L)] x_1^2 x_2 \\ & + DI^2 [DG(4K+7L) + HL(2K+L) + DH(K+2L)] x_1 x_2^2 + 2D^4 K(G+H)x_1 + 2D^4 ILx_2 \\ & + D^2 I [D(K+L)(5G+3H) + 2HKL] x_1 x_2 + (D^2 + DGx_1 + DIx_2 + GIx_1 x_2) (GKx_1 - ILx_2)^2. \end{aligned}$$

Thus, $r_1 > 0$. Consequently, the conditions [\(B.8\)](#) are satisfied. Finally, SS8 is stable if and only if $\lambda_1 < 0$, that is to say $\mu_0(s_0^{\text{in}}, M_2(D+a_2)) < D+a_0$. Since M_0 is increasing, this condition is equivalent to the stability condition of SS8 in [Table 5](#).

B.2. Proof of Proposition 3.3. If SS2 exists then, its condition of existence $\mu_2(s_2^{\text{in}}) > D+a_2$ holds. Therefore, the condition $\mu_2(s_2^{\text{in}}) < D+a_2$ of stability of SS1 is not satisfied.

If SS3 exists then, its condition of existence $\mu_0(s_0^{\text{in}}, s_2^{\text{in}}) > D+a_0$ holds. Therefore, the condition $\mu_0(s_0^{\text{in}}, s_2^{\text{in}}) < D+a_0$ of stability of SS1 is not satisfied.

If SS7 exists then, its condition of existence $\mu_1(s_1^{\text{in}}, s_2^{\text{in}}) > D+a_1$ holds. Therefore, the condition $\mu_1(s_1^{\text{in}}, s_2^{\text{in}}) < D+a_1$ of stability of SS1 is not satisfied.

If SS6 exists then, the conditions

$$(1-\omega)s_0^{\text{in}} + s_1^{\text{in}} + s_2^{\text{in}} > \phi_2(D), \quad s_0^{\text{in}} > \varphi_0(D), \quad s_0^{\text{in}} + s_1^{\text{in}} > \varphi_0(D) + \varphi_1(D)$$

hold. Therefore, the condition $s_0^{\text{in}} < \varphi_0(D)$ of stability of SS2 or SS8 is not satisfied, the condition $(1-\omega)s_0^{\text{in}} + s_1^{\text{in}} + s_2^{\text{in}} < \phi_2(D)$ of stability of SS4 is not satisfied, and the condition $s_0^{\text{in}} + s_1^{\text{in}} < \varphi_0(D) + \varphi_1(D)$ of stability of SS5 is not satisfied.

If SS5 exists then, its conditions of existence

$$s_0^{\text{in}} > \varphi_0(D) \quad \text{and} \quad s_2^{\text{in}} - \omega s_0^{\text{in}} > M_2(D+a_2) - \omega \varphi_0(D)$$

hold. Therefore, the condition $s_0^{\text{in}} < \varphi_0(D)$ of stability of SS2 or SS8 is not satisfied and the condition $s_2^{\text{in}} - \omega s_0^{\text{in}} < M_2(D+a_2) - \omega \varphi_0(D)$ of stability of SS3 is not satisfied.

If SS8 exists then, its conditions of existence $s_1^{\text{in}} + s_2^{\text{in}} > \varphi_1(D) + M_2(D+a_2)$ holds. Therefore, the condition $s_1^{\text{in}} + s_2^{\text{in}} < \varphi_1(D) + M_2(D+a_2)$ of stability of SS7 is not satisfied.

Appendix C. Proof of Proposition 4.1. We assume that the biological parameter values in model [\(4.1\)](#) are provided in [Table 14](#). We assume that $S_{\text{ph}}^{\text{in}} = 0$, $S_{\text{H}_2}^{\text{in}} = 2.67 \times 10^{-5}$ as in [Fig. 3\(a\)](#) from [\[24\]](#). We assume that $D = 0.01$. As said in [Section 4, Theorem 3.1](#) applies to model [\(4.1\)](#). From [Table 2](#), SS7 and SS8 do not exist when $s_1^{\text{in}} = 0$. Using the change of variables [\(E.2\)](#), the necessary and sufficient existence and stability conditions of steady states of [\(4.1\)](#), as stated in [Tables 2 and 5](#), are summarized in [Table 11](#). Since the second stability condition of SS1 in [Table 11](#) does not hold

$$(C.1) \quad \mu_2(S_{\text{H}_2}^{\text{in}}) \simeq 1.0845 > D + a_2 = 0.03,$$

TABLE 11

Existence and local stability conditions of steady states of (4.1), when $S_{\text{ph}}^{\text{in}} = 0$. The functions ϕ_4 and μ_i are given in Table 3 and (E.3) while c_3, c_5, r_4 and r_5 are defined by Table 4. All other functions are given in Table 10 and Table 15.

	Existence conditions	Stability conditions
SS1	Always exists	$\mu_0 (Y S_{\text{ch}}^{\text{in}}, S_{\text{H}_2}^{\text{in}}) < D + a_0, \mu_2 (S_{\text{H}_2}^{\text{in}}) < D + a_2$
SS2	$\mu_2 (S_{\text{H}_2}^{\text{in}}) > D + a_2$	$Y S_{\text{ch}}^{\text{in}} < \varphi_0(D)$
SS3	$\mu_0 (Y S_{\text{ch}}^{\text{in}}, S_{\text{H}_2}^{\text{in}}) > D + a_0$	$\mu_1 (Y S_{\text{ch}}^{\text{in}} - s_0, S_{\text{H}_2}^{\text{in}} + \omega (Y S_{\text{ch}}^{\text{in}} - s_0)) < D + a_1$ $S_{\text{H}_2}^{\text{in}} - \omega Y S_{\text{ch}}^{\text{in}} < M_2(D + a_2) - \omega \varphi_0(D)$ with s_0 solution of $\psi_0(s_0) = D + a_0$
SS4	$(1 - \omega)Y S_{\text{ch}}^{\text{in}} + S_{\text{H}_2}^{\text{in}} \geq \phi_1(D)$, $Y S_{\text{ch}}^{\text{in}} > M_0(D + a_0, s_2) + M_1(D + a_1, s_2)$ with s_2 solution of $\Psi(s_2, D) = (1 - \omega)Y S_{\text{ch}}^{\text{in}} + S_{\text{H}_2}^{\text{in}}$	$(1 - \omega)Y S_{\text{ch}}^{\text{in}} + S_{\text{H}_2}^{\text{in}} < \phi_2(D), \phi_3(D) > 0$ $\frac{\partial \Psi}{\partial s_2}(s_2, D) > 0, \phi_4(D, S_{\text{ch}}^{\text{in}}, S_{\text{H}_2}^{\text{in}}) > 0$
SS5	$Y S_{\text{ch}}^{\text{in}} > \varphi_0(D)$, $S_{\text{H}_2}^{\text{in}} - \omega Y S_{\text{ch}}^{\text{in}} > M_2(D + a_2) - \omega \varphi_0(D)$	$Y S_{\text{ch}}^{\text{in}} < \varphi_0(D) + \varphi_1(D)$
SS6	$(1 - \omega)Y S_{\text{ch}}^{\text{in}} + S_{\text{H}_2}^{\text{in}} > \phi_2(D)$, $Y S_{\text{ch}}^{\text{in}} > \varphi_0(D) + \varphi_1(D)$	$c_3 > 0, c_5 > 0, r_4 > 0, r_5 > 0$

SS1 always exists and is unstable. Since the existence condition of SS2 in Table 11 holds (see inequality (C.1)), SS2 exists and is stable if and only if

$$S_{\text{ch}}^{\text{in}} < \varphi_0(D)/Y =: \sigma_3.$$

SS3 exists if and only if

$$S_{\text{ch}}^{\text{in}} > M_0(D + a_0, S_{\text{H}_2}^{\text{in}})/Y =: \sigma_1.$$

Let $F(S_{\text{ch}}^{\text{in}})$ be the function defined by

$$(C.2) \quad F(S_{\text{ch}}^{\text{in}}) = \mu_1(S_{\text{ch}}^{\text{in}}Y - s_0, S_{\text{H}_2}^{\text{in}} + \omega(S_{\text{ch}}^{\text{in}}Y - s_0)).$$

The first stability condition of SS3 in Table 11 holds for all $S_{\text{ch}}^{\text{in}} > \sigma_1$, that is, $F(S_{\text{ch}}^{\text{in}}) < D + a_1$ since the maximum of F is smaller than 0.0013 while $D + a_1 = 0.03$ (see Figure C.1). From the second stability condition in Table 11, SS3 is stable if and only if

$$S_{\text{ch}}^{\text{in}} > (S_{\text{H}_2}^{\text{in}} - M_2(D + a_2) + \omega \varphi_0(D)) / (\omega Y) =: \sigma_4.$$

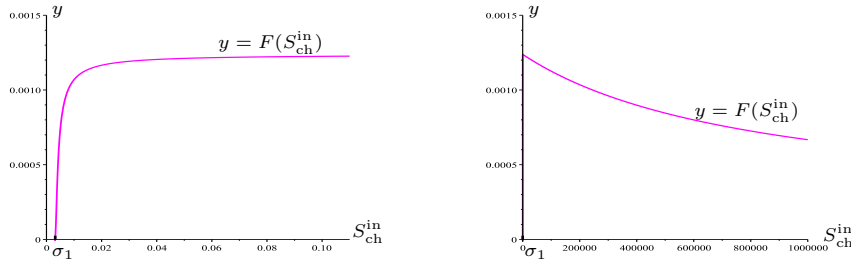


FIG. C.1. Curve of the function $y = F(S_{\text{ch}}^{\text{in}})$ defined by (C.2).

From Theorem 2.1, the system can have at most two steady states of the form SS4 denoted by SS4¹ and SS4² as $\omega \simeq 0.53 < 1$. Their first existence condition in Table 11 holds if and only if

$$S_{\text{ch}}^{\text{in}} \geq (\phi_1(D) - S_{\text{H}_2}^{\text{in}}) / ((1 - \omega)Y) =: \sigma_2.$$

Their second existence condition holds, for all $S_{\text{ch}}^{\text{in}} \in [\sigma_2, 0.11]$, since the straight line of equation $y = S_{\text{ch}}^{\text{in}} Y$ is above the curves of the functions $y = M_0(D + a_0, s_2^{*i}) + M_1(D + a_1, s_2^{*i})$, for $i = 1, 2$, respectively (see [Figure C.2](#)). Thus, SS4^1 and SS4^2 exist and are unstable for all $S_{\text{ch}}^{\text{in}} \geq \sigma_2$ since the second stability condition does not hold where $\phi_3(D) \simeq -1996.917 < 0$.

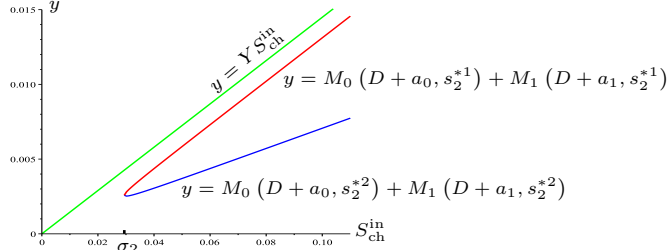


FIG. C.2. The green line of equation $y = Y S_{\text{ch}}^{\text{in}}$ is above the red and blue curves of the functions $M_0(D + a_0, s_2^{*i}) + M_1(D + a_1, s_2^{*i})$, for $i = 1, 2$, which correspond to SS4^1 and SS4^2 , respectively.

SS5 exists if and only if

$$\sigma_3 := \varphi_0(D)/Y < S_{\text{ch}}^{\text{in}} < (S_{\text{H}_2}^{\text{in}} - M_2(D + a_2) + \omega\varphi_0(D)) / (\omega Y) =: \sigma_4.$$

When it exists, SS5 is stable since

$$S_{\text{ch}}^{\text{in}} < \sigma_4 \simeq 0.013985 < (\varphi_0(D) + \varphi_1(D))/Y \simeq 0.02304.$$

SS6 exists if and only if

$$S_{\text{ch}}^{\text{in}} > \frac{\phi_2(D) - S_{\text{H}_2}^{\text{in}}}{(1-\omega)Y} =: \sigma_5 \simeq 0.033292, \quad S_{\text{ch}}^{\text{in}} > \frac{\varphi_0(D) + \varphi_1(D)}{Y} \simeq 0.02304.$$

Hence, SS6 exists if and only if $S_{\text{ch}}^{\text{in}} > \sigma_5$. To determine the stability of SS6 , the functions c_3 , c_5 , r_4 and r_5 are plotted with respect to $S_{\text{ch}}^{\text{in}} > \sigma_5$. [Figure C.3](#) shows that $c_3(S_{\text{ch}}^{\text{in}})$, $c_5(S_{\text{ch}}^{\text{in}})$, $r_4(S_{\text{ch}}^{\text{in}})$ and $r_5(S_{\text{ch}}^{\text{in}})$ are all positive if and only if $S_{\text{ch}}^{\text{in}} > \sigma_6$ where $\sigma_6 \simeq 0.1025$ is the largest root of equation $r_5(S_{\text{ch}}^{\text{in}}) = 0$. To show that the positive steady state SS6 is destabilized due to Hopf bifurcation for $S_{\text{ch}}^{\text{in}} = \sigma_6$, we determine numerically the eigenvalues of the Jacobian matrix of system [\(4.1\)](#) at SS6 and we plot them with respect to $S_{\text{ch}}^{\text{in}}$. [Figure C.4\(a-b\)](#) shows that two eigenvalues denoted by $\lambda_1(S_{\text{ch}}^{\text{in}})$ and $\lambda_2(S_{\text{ch}}^{\text{in}})$ are real and remain negative for all $S_{\text{ch}}^{\text{in}} \in (\sigma_5, 0.11]$. [Figure C.4\(c\)](#) shows that the two other eigenvalues $\lambda_3(S_{\text{ch}}^{\text{in}})$ and $\lambda_4(S_{\text{ch}}^{\text{in}})$ are real, negative and distinct for all $S_{\text{ch}}^{\text{in}} \in (\sigma_5, \sigma^*)$ where $\sigma^* \simeq 0.03467$. Then, they become a complex-conjugate pair denoted by

$$\lambda_{3,4}(S_{\text{ch}}^{\text{in}}) = \alpha_{3,4}(S_{\text{ch}}^{\text{in}}) \pm i\beta_{3,4}(S_{\text{ch}}^{\text{in}}), \quad \text{for all } S_{\text{ch}}^{\text{in}} \in (\sigma^*, 0.11)$$

where the real part $\alpha_{3,4}$ remains negative. [Figure C.4\(d\)](#) shows that the two last eigenvalues $\lambda_5(S_{\text{ch}}^{\text{in}})$ and $\lambda_6(S_{\text{ch}}^{\text{in}})$ are real, negative and distinct for all $S_{\text{ch}}^{\text{in}} \in (\sigma_5, \sigma^*)$. Then, they become a complex-conjugate pair denoted by

$$\lambda_{5,6}(S_{\text{ch}}^{\text{in}}) = \alpha_{5,6}(S_{\text{ch}}^{\text{in}}) \pm i\beta_{5,6}(S_{\text{ch}}^{\text{in}}), \quad \text{for all } S_{\text{ch}}^{\text{in}} \in (\sigma^*, 0.11).$$

At the particular value $S_{\text{ch}}^{\text{in}} = \sigma_6$, the pair $\lambda_{5,6}(S_{\text{ch}}^{\text{in}})$ is purely imaginary such that $\alpha_{5,6}(\sigma_6) = 0$, with $\beta_{5,6}(\sigma_6) \neq 0$. Moreover, one has

$$\frac{d\alpha_{5,6}}{dS_{\text{ch}}^{\text{in}}}(\sigma_6) < 0.$$

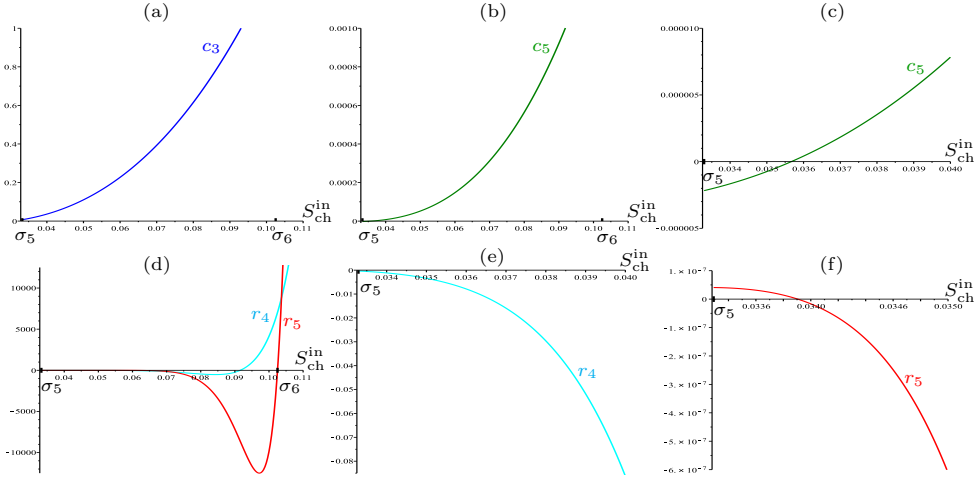


FIG. C.3. Curves of the functions $c_3(S_{\text{ch}}^{\text{in}})$, $c_5(S_{\text{ch}}^{\text{in}})$, $r_4(S_{\text{ch}}^{\text{in}})$ and $r_5(S_{\text{ch}}^{\text{in}})$ for $S_{\text{ch}}^{\text{in}} > \sigma_5$. (a) Curve of c_3 . (b) Curve of c_5 . (c) Magnification of the curve of c_5 . (d) Curves of r_4 and r_5 . (e) Magnification of the curve of r_4 . (f) Magnification of the curve of r_5 .

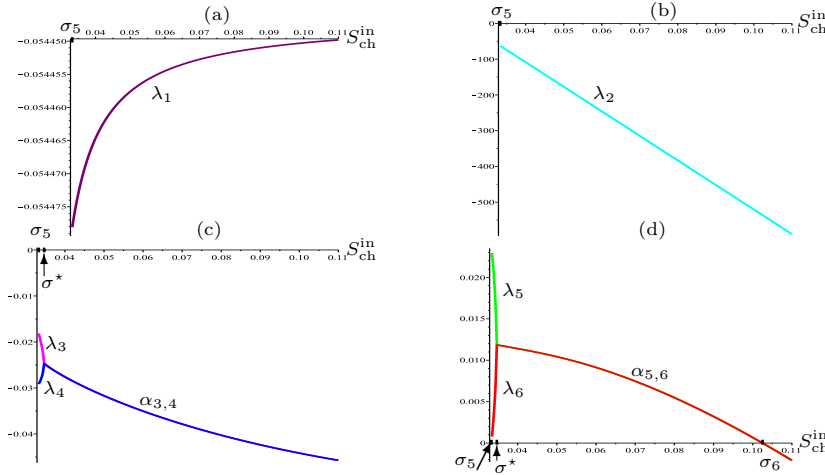


FIG. C.4. The real part of the eigenvalues of the Jacobian matrix at SS6 as a function of $S_{\text{ch}}^{\text{in}}$, when $D = 0.01$, $S_{\text{ph}}^{\text{in}} = 0$ and $S_{\text{H}_2}^{\text{in}} = 2.67 \times 10^{-5}$. The real parts $\alpha_{3,4}$ and $\alpha_{5,6}$ for $S_{\text{ch}}^{\text{in}} \in (\sigma^*, 0.11]$.

Therefore, SS6 changes its stability through a supercritical Hopf bifurcation with the emergence of a stable limit cycle that we illustrate in [Figures 4.5](#) and [F.1](#).

Remark C.1. Note that [Figures C.1](#) and [C.2](#) showing the stability of SS3 and the existence of two steady states of type SS4 are similar to [Figures 6](#) and [7](#) in [\[15\]](#), respectively. But, on the contrary, [Figure C.3](#) which concerns the stability of SS6 is completely different from [Figure 8](#) in [\[15\]](#), since the conditions of stability of SS6 require to consider the signs of the Liénard-Chipart coefficients c_3 , c_5 , r_3 and r_5 .

Appendix D. Liénard-Chipart stability criteria.

Lemma D.1. Consider the fourth-order polynomial $\tilde{P}_4(\lambda)$ with real coefficients given by:

$$\tilde{P}_4(\lambda) = c_0\lambda^4 + c_1\lambda^3 + c_2\lambda^2 + c_3\lambda + c_4.$$

All of the roots of the polynomial $\tilde{P}_4(\lambda)$ have negative real part if and only if

$$(D.1) \quad c_i > 0, \quad \text{for } i = 1, 3, 4, \quad \text{and } r_1 = c_3 r_0 - c_1^2 c_4 > 0,$$

where $r_0 = c_1 c_2 - c_0 c_3$.

Proof. From the Liénard-Chipart stability criteria (see Gantmacher [9], Theorem 11), all of the roots of the polynomial \tilde{P}_4 have negative real part if and only if

$$(D.2) \quad c_i > 0, \quad i = 1, 3, 4, \quad \det(\Delta_2) > 0 \quad \text{and} \quad \det(\Delta_4) > 0,$$

where Δ_2 and Δ_4 are the Hurwitz matrices defined by:

$$\Delta_2 = \begin{bmatrix} c_1 & c_3 \\ c_0 & c_2 \end{bmatrix} \quad \text{and} \quad \Delta_4 = \begin{bmatrix} c_1 & c_3 & 0 & 0 \\ c_0 & c_2 & c_4 & 0 \\ 0 & c_1 & c_3 & 0 \\ 0 & c_0 & c_2 & c_4 \end{bmatrix}.$$

Conditions (D.2) are equivalent to

$$(D.3) \quad c_i > 0, \quad i = 1, 3, 4, \quad r_0 = c_1 c_2 - c_0 c_3 > 0 \quad \text{and} \quad r_1 = c_3 r_0 - c_1^2 c_4 > 0.$$

When all conditions (D.3) hold, the condition $r_1 > 0$ implies that $r_0 > 0$. Thus, conditions (D.3) are equivalent to (D.1). \square

Lemma D.2. Consider the six-order polynomial $\tilde{P}_6(\lambda)$ with real coefficients given by:

$$\tilde{P}_6(\lambda) = c_0 \lambda^6 + c_1 \lambda^5 + c_2 \lambda^4 + c_3 \lambda^3 + c_4 \lambda^2 + c_5 \lambda + c_6.$$

All of the roots of the polynomial $\tilde{P}_6(\lambda)$ have negative real part if and only if

$$(D.4) \quad c_i > 0, \quad i = 1, 3, 5, 6, \quad r_4 > 0 \quad \text{and} \quad r_5 > 0,$$

where $r_4 = r_1 r_2 - r_0 r_3$ and $r_5 = r_3 r_4 - c_1 c_6 r_2^2$, with

$$r_0 = c_1 c_2 - c_0 c_3, \quad r_1 = c_1 c_4 - c_0 c_5, \quad r_2 = c_3 r_0 - c_1 r_1 \quad \text{and} \quad r_3 = c_5 r_0 - c_1^2 c_6.$$

Proof. From the Liénard-Chipart stability criteria (see Gantmacher [9], Theorem 11), all of the roots of the polynomial \tilde{P}_6 have negative real part if and only if

$$(D.5) \quad c_i > 0, \quad i = 1, 3, 5, 6, \quad \det(\Delta_2) > 0, \quad \det(\Delta_4) > 0 \quad \text{and} \quad \det(\Delta_6) > 0,$$

where Δ_2 , Δ_4 and Δ_6 are the Hurwitz matrices defined by:

$$\Delta_2 = \begin{bmatrix} c_1 & c_3 \\ c_0 & c_2 \end{bmatrix}, \quad \Delta_4 = \begin{bmatrix} c_1 & c_3 & c_5 & 0 \\ c_0 & c_2 & c_4 & c_6 \\ 0 & c_1 & c_3 & c_5 \\ 0 & c_0 & c_2 & c_4 \end{bmatrix}, \quad \Delta_6 = \begin{bmatrix} c_1 & c_3 & c_5 & 0 & 0 & 0 \\ c_0 & c_2 & c_4 & c_6 & 0 & 0 \\ 0 & c_1 & c_3 & c_5 & 0 & 0 \\ 0 & c_0 & c_2 & c_4 & c_6 & 0 \\ 0 & 0 & c_1 & c_3 & c_5 & 0 \\ 0 & 0 & c_0 & c_2 & c_4 & c_6 \end{bmatrix}.$$

Conditions (D.5) are equivalent to

$$(D.6) \quad c_i > 0, \quad i = 1, 3, 5, 6, \quad r_0 > 0, \quad r_4 = r_1 r_2 - r_0 r_3 > 0, \quad r_5 = r_3 r_4 - c_1 c_6 r_2^2 > 0.$$

When all conditions (D.6) hold, the condition $r_5 > 0$ implies that $r_3 > 0$, that is, $c_5 r_0 > c_6 c_1^2$ which implies that $r_0 > 0$. Hence, conditions (D.6) are equivalent to (D.4). \square

Appendix E. A chlorophenol-mineralising three-tiered microbial 'food web'. Following [19], model (4.1) can be written in the form of model (1.1), using the following change of variables:

$$(E.1) \quad x_0 = \frac{Y}{Y_0} X_{\text{ch}}, x_1 = \frac{Y_4}{Y_1} X_{\text{ph}}, x_2 = \frac{1}{Y_2} X_{\text{H}_2}, s_0 = Y S_{\text{ch}}, s_1 = Y_4 S_{\text{ph}}, s_2 = S_{\text{H}_2},$$

where $Y = Y_3 Y_4$. The input concentrations are given by:

$$(E.2) \quad s_0^{\text{in}} = Y S_{\text{ch}}^{\text{in}}, \quad s_1^{\text{in}} = Y_4 S_{\text{ph}}^{\text{in}}, \quad s_2^{\text{in}} = S_{\text{H}_2}^{\text{in}},$$

the death rates are $a_0 = k_{\text{dec, ch}}$, $a_1 = k_{\text{dec, ph}}$, $a_2 = k_{\text{dec, H}_2}$, and the yield coefficients are

$$Y_0 = Y_{\text{ch}}, \quad Y_1 = Y_{\text{ph}}, \quad Y_2 = Y_{\text{H}_2}, \quad Y_3 = 224/208(1 - Y_0), \quad Y_4 = 32/224(1 - Y_1)$$

with $\omega = \frac{16}{208Y} = \frac{1}{2(1-Y_{\text{ch}})(1-Y_{\text{ph}})}$. The specific growth functions (4.2) become the following functions satisfying Hypotheses (H1) to (H8):

$$(E.3) \quad \mu_0(s_0, s_2) = \frac{m_0 s_0}{K_0 + s_0} \frac{s_2}{L_0 + s_2}, \quad \mu_1(s_1, s_2) = \frac{m_1 s_1}{K_1 + s_1} \frac{1}{1 + s_2/K_I}, \quad \mu_2(s_2) = \frac{m_2 s_2}{K_2 + s_2},$$

where

$$m_0 = Y_0 k_{m, \text{ch}}, \quad K_0 = Y K_{S, \text{ch}}, \quad L_0 = K_{S, \text{H}_2, \text{c}}, \quad m_1 = Y_1 k_{m, \text{ph}}, \\ K_1 = Y_4 K_{S, \text{ph}}, \quad K_I = K_{I, \text{H}_2}, \quad m_2 = Y_2 k_{m, \text{H}_2}, \quad K_2 = K_{S, \text{H}_2}.$$

For these specific kinetics (E.3), the various functions defined in Table 10 are listed in Table 15. Using the linear change of variable given by (E.1) and (E.2), the yield coefficients in (4.1) are normalized to one except one of them, which is equal to $\omega \simeq 0.53$, when the yield coefficients are those given in Table 14. Therefore, (4.1) is of the form (1.1), with $\omega < 1$ and the results of our paper apply to (4.1).

The aim of this section is to give rigorous proofs for the results of [24] on existence and stability of the steady states of model (4.1). Notice that the results in [24] were given with respect to the dimensionless form (F.2) of (4.1) by using the variables (F.1) and the growth functions (F.3). The variables (F.1) are related to our variables (E.1) by the formulas

$$x_0 = X_0 K_0, \quad x_1 = X_1 K_1, \quad x_2 = X_2 K_2, \quad s_0 = S_0 K_0, \quad s_1 = S_1 K_1, \quad s_2 = S_2 K_2, \quad t = \tau/m_0.$$

Hence, results given in variables (F.1) can be easily translated into results given in variables (E.1) and vice versa.

From Tables 2 and 5, the existence and stability of steady states of model (4.1) can be determine for the specific growth functions (E.3). Using the functions and notations given in Table 15, we have the following results:

SS1 = $(0, 0, 0, s_0^{\text{in}}, s_1^{\text{in}}, s_2^{\text{in}})$ always exists. It is stable if and only if

$$\mu_0(s_0^{\text{in}}, s_2^{\text{in}}) < D + a_0, \quad \mu_1(s_1^{\text{in}}, s_2^{\text{in}}) < D + a_1 \quad \text{and} \quad \mu_2(s_2^{\text{in}}) < D + a_2.$$

These conditions are equivalent to the conditions of [24], section C1, given in terms of variables (F.1) and growth functions (F.3).

SS2 = $(0, 0, x_2, s_0, s_1, s_2)$ is given by:

$$(E.4) \quad s_0 = s_0^{\text{in}}, \quad s_1 = s_1^{\text{in}}, \quad s_2 = \frac{K_2(D+a_2)}{m_2-D-a_2}, \quad x_2 = \frac{D}{D+a_2} (s_2^{\text{in}} - s_2).$$

It exists if and only if $s_2^{\text{in}} > s_2$, where s_2 is given by (E.4). It is stable if and only if

$$\mu_0(s_0^{\text{in}}, s_2) < D + a_0 \quad \text{and} \quad \mu_1(s_1^{\text{in}}, s_2) < D + a_1.$$

Formulas (E.4) together with the conditions of existence and stability of SS2 were established in [24], section C2, using variables (F.1) and growth functions (F.3).

SS3 = $(x_0, 0, 0, s_0, s_1, s_2)$ is given by:

$$(E.5) \quad x_0 = \frac{D}{D+a_0}(s_0^{\text{in}} - s_0), \quad s_1 = s_1^{\text{in}} + s_0^{\text{in}} - s_0, \quad s_2 = s_2^{\text{in}} - \omega(s_0^{\text{in}} - s_0),$$

where s_0 is a solution of equation

$$(E.6) \quad \frac{m_0 s_0 (s_2^{\text{in}} - \omega(s_0^{\text{in}} - s_0))}{(K_0 + s_0)(L_0 + s_2^{\text{in}} - \omega(s_0^{\text{in}} - s_0))} = D + a_0.$$

Notice that (E.6) is a quadratic equation. Only its solution in the interval

$$J_0 = [\max(0, s_0^{\text{in}} - s_2^{\text{in}}/\omega), s_0^{\text{in}})$$

is to be considered. SS3 exists if and only if the following condition holds

$$(E.7) \quad \mu_0(s_0^{\text{in}}, s_2^{\text{in}}) > D + a_0.$$

It is stable if and only if

$$(E.8) \quad \begin{aligned} \mu_1(s_0^{\text{in}} - s_0 + s_1^{\text{in}}, s_2^{\text{in}} - \omega(s_0^{\text{in}} - s_0)) &< D + a_1, \\ s_2^{\text{in}} - \omega s_0^{\text{in}} &< M_2(D + a_2) - \omega M_0(D + a_0, M_2(D + a_2)), \end{aligned}$$

where s_0 is the solution in the interval J_0 of equation (E.6). Formulas (E.5) together with equation (E.6) giving s_0 and the stability condition (E.8) were established in [24], section C3, using variables (F.1) and growth functions (F.3). However, neither condition (E.7) of existence of SS3 nor the signs of other eigenvalues of the Jacobian matrix were explicitly established in [24], section C3, where the existence and stability of SS3 were checked only numerically by considering the roots of polynomials of degrees 2 and 3, respectively, see formulas (C.3) and (C.7) in [24].

SS4 = $(x_0, x_1, 0, s_0, s_1, s_2)$ is given by:

$$(E.9) \quad \begin{aligned} s_0 &= \frac{(D+a_0)K_0(L_0+s_2)}{m_0 s_2 - (D+a_0)(L_0+s_2)}, \quad s_1 = \frac{(D+a_1)K_1(K_I+s_2)}{m_1 K_I - (D+a_1)(K_I+s_2)}, \\ x_0 &= \frac{D}{D+a_0}(s_0^{\text{in}} - s_0), \quad x_1 = \frac{D}{D+a_1}(s_0^{\text{in}} - s_0 + s_1^{\text{in}} - s_1), \end{aligned}$$

where s_2 is a solution of equation

$$(E.10) \quad \begin{aligned} (1 - \omega) \frac{(D+a_0)K_0(L_0+s_2)}{m_0 s_2 - (D+a_0)(L_0+s_2)} + \frac{(D+a_1)K_1(K_I+s_2)}{m_1 K_I - (D+a_1)(K_I+s_2)} + s_2 \\ = (1 - \omega)s_0^{\text{in}} + s_1^{\text{in}} + s_2^{\text{in}}. \end{aligned}$$

Notice that (E.10) reduces to a cubic equation in s_2 . Only its solutions in the interval (s_2^0, s_2^1) are to be considered. The steady states SS4¹ and SS4² exist if and only if the following conditions hold

$$(E.11) \quad s_0^{\text{in}} > s_0, \quad s_0^{\text{in}} + s_1^{\text{in}} > s_0 + s_1 \quad \text{and} \quad (1 - \omega)s_0^{\text{in}} + s_1^{\text{in}} + s_2^{\text{in}} \geq \phi_1(D),$$

where s_0 and s_1 are defined by (E.9). $SS4^1$ is unstable whenever it exists and $SS4^2$ is stable if and only if

$$(E.12) \quad (1 - \omega)s_0^{\text{in}} + s_1^{\text{in}} + s_2^{\text{in}} < \phi_2(D), \quad \phi_3(D) > 0 \quad \text{and} \quad \phi_4(D, s_0^{\text{in}}, s_1^{\text{in}}, s_2^{\text{in}}) > 0.$$

Here ϕ_2 and ϕ_3 are defined in Table 10, and ϕ_4 is defined in Table 3. Formulas (E.9) together with equation (E.10) giving s_2 were established in [24], section C4, using variables (F.1) and growth functions (F.3). However, neither condition (E.11) of existence of $SS4$ nor its condition of stability (E.12) have been established explicitly in [24], section C4, where the existence and stability of $SS4$ were checked only numerically by considering the roots of a polynomial of degree 5, see formula (C.20) in [24].

$SS5 = (x_0, 0, x_2, s_0, s_1, s_2)$ is given by:

$$(E.13) \quad \begin{aligned} s_2 &= \frac{(D+a_2)K_2}{m_2-D-a_2}, & s_0 &= \frac{(D+a_0)K_0(L_0+s_2)}{m_0s_2-(D+a_0)(L_0+s_2)}, & s_1 &= s_0^{\text{in}} - s_0 + s_1^{\text{in}}, \\ x_0 &= \frac{D}{D+a_0}(s_0^{\text{in}} - s_0), & x_2 &= \frac{D}{D+a_2}(s_2^{\text{in}} - s_2 - \omega(s_0^{\text{in}} - s_0)). \end{aligned}$$

It exists if and only if the following conditions hold

$$(E.14) \quad s_0^{\text{in}} > s_0, \quad s_2^{\text{in}} - \omega s_0^{\text{in}} > s_2 - \omega s_0.$$

where s_0 and s_2 are given by (E.13). $SS5$ is stable if and only if

$$(E.15) \quad s_0^{\text{in}} + s_1^{\text{in}} < M_0(D + a_0, M_2(D + a_2)) + M_1(D + a_1, M_2(D + a_2)).$$

Formulas (E.13) together with conditions (E.14) of existence and (E.15) of stability of $SS5$ were established in [24], section C5, using variables (F.1) and growth functions (F.3). However, the signs of other eigenvalues of the Jacobian matrix have been checked only numerically by considering the roots of a polynomial of degree 4, see formula (C.31) in [24].

$SS6 = (x_0, x_1, x_2, s_0, s_1, s_2)$ is given by:

$$(E.16) \quad \begin{aligned} s_2 &= \frac{(D+a_2)K_2}{m_2-D-a_2}, & s_0 &= \frac{(D+a_0)K_0(L_0+s_2)}{m_0s_2-(D+a_0)(L_0+s_2)}, & s_1 &= \frac{(D+a_1)K_1(K_I+s_2)}{m_1K_I-(D+a_1)(K_I+s_2)}, \\ x_0 &= \frac{D}{D+a_0}(s_0^{\text{in}} - s_0), & x_1 &= \frac{D}{D+a_1}(s_0^{\text{in}} - s_0 + s_1^{\text{in}} - s_1), \\ x_2 &= \frac{D}{D+a_2}((1 - \omega)(s_0^{\text{in}} - s_0) + s_1^{\text{in}} - s_1 + s_2^{\text{in}} - s_2). \end{aligned}$$

It exists if and only if the following conditions hold

$$(E.17) \quad s_0^{\text{in}} > s_0, \quad s_0^{\text{in}} + s_1^{\text{in}} > s_0 + s_1, \quad (1 - \omega)s_0^{\text{in}} + s_1^{\text{in}} + s_2^{\text{in}} > \phi_2(D),$$

where s_0 and s_1 are given by (E.16). $SS6$ is stable if and only if

$$(E.18) \quad c_i > 0, \quad i = 3, 5, \quad \text{and} \quad r_j > 0, \quad j = 4, 5,$$

where c_i and r_j are defined in Table 4. Formulas (E.16) together with conditions (E.17) of existence of $SS6$ were established in [24], section C6, using variables (F.1) and growth functions (F.3). However, the Liénard-Chipart stability conditions (E.18) were not considered in [24], where the stability of $SS6$ was checked only numerically by considering the roots of a polynomial of degree 6, see formula (C.42) in [24].

$SS7 = (0, x_1, 0, s_0, s_1, s_2)$ is given by:

$$(E.19) \quad s_0 = s_0^{\text{in}}, \quad x_1 = \frac{D}{D+a_1}(s_1^{\text{in}} - s_1), \quad s_2 = s_1^{\text{in}} - s_1 + s_2^{\text{in}},$$

where s_1 is a unique solution of equation

$$(E.20) \quad \frac{m_1 s_1 K_I}{(K_1 + s_1)(K_I + s_1^{\text{in}} + s_2^{\text{in}} - s_1)} = D + a_1.$$

Notice that (E.20) is a quadratic equation. Only its solution in the interval

$$J_1 = [0, s_1^{\text{in}})$$

is to be considered. SS7 exists if and only if the following condition holds

$$(E.21) \quad \mu_1(s_1^{\text{in}}, s_2^{\text{in}}) > D + a_1.$$

SS7 is stable if and only if

$$(E.22) \quad \begin{aligned} s_1^{\text{in}} + s_2^{\text{in}} &< M_1(D + a_1, M_3(s_0^{\text{in}}, D + a_0)) + M_3(s_0^{\text{in}}, D + a_0), \\ s_1^{\text{in}} + s_2^{\text{in}} &< M_1(D + a_1, M_2(D + a_2)) + M_2(D + a_2). \end{aligned}$$

Formulas (E.19) together with equation (E.20) giving s_1 and stability condition (E.22) were established in [24], section C7, using variables (F.1) and growth functions (F.3). However, condition (E.21) of existence of SS7 has not been established explicitly in [24], section C7, where the existence of SS7 and the signs of other eigenvalues of the Jacobian matrix were checked only numerically by considering the roots of a polynomial of degree 3, see formula (C.53) in [24].

SS8 = (0, x_1, x_2, s_0, s_1, s_2) is given by:

$$(E.23) \quad \begin{aligned} s_0 &= s_0^{\text{in}}, \quad s_2 = \frac{(D+a_2)K_2}{m_2 - D - a_2}, \quad s_1 = \frac{(D+a_1)K_1(K_I + s_2)}{m_1 K_I - (D+a_1)(K_I + s_2)}, \\ x_1 &= \frac{D}{D+a_1}(s_1^{\text{in}} - s_1), \quad x_2 = \frac{D}{D+a_2}(s_1^{\text{in}} - s_1 + s_2^{\text{in}} - s_2). \end{aligned}$$

It exists if and only if the following conditions hold

$$(E.24) \quad s_1^{\text{in}} > s_1, \quad s_1^{\text{in}} + s_2^{\text{in}} > s_1 + s_2,$$

where s_1 and s_2 are given by (E.23). SS8 is stable if and only if

$$(E.25) \quad s_0^{\text{in}} < M_0(D + a_0, M_2(D + a_2)).$$

Formulas (E.23) together with conditions (E.24) of existence and (E.25) of stability of SS8 were established in [24], section C8, using variables (F.1) and growth functions (F.3). However, the signs of other eigenvalues of the Jacobian matrix have been checked only numerically by considering the roots of a polynomial of degree 4, see formula (C.62) in [24].

Appendix F. Numerical simulations. The plots of Figures C.1 to C.4 were performed with Maple [10], which is used in particular for the computations of coefficients c_3, c_5, r_4 and r_5 , evaluated at SS6, and the computations of the eigenvalues of the Jacobian matrix evaluated at SS6. The plots of Figures 4.1 to 4.3 were performed with Scilab [21] by using the formulas of the steady state components given in Table 1. The various functions appearing in these formulas are given in Table 15. The plots of Figures 4.4 to 4.6 and F.1 to F.4 were performed with Scilab [21]. The numerical simulations presented in Figures 4.4 to 4.6, C.4, and F.1 to F.4 were performed on the dimensionless form of (4.1) used in [24]. Indeed, in the original form (4.1), numerical instabilities arise in numerical schemes. To reduce the number of parameters

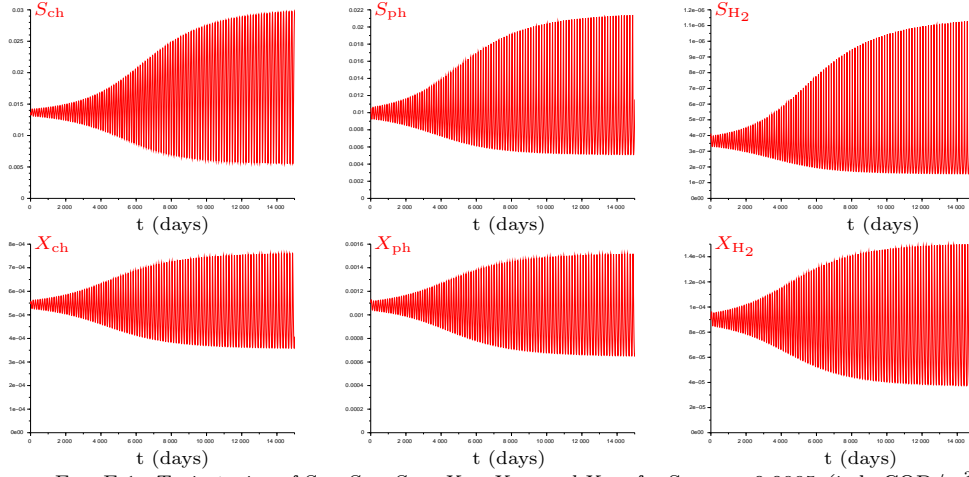


FIG. F.1. Trajectories of S_{ch} , S_{ph} , S_{H_2} , X_{ch} , X_{ph} and X_{H_2} for $S_{ch,in} = 0.0995$ (in kgCOD/m^3): Convergence to the stable limit cycle.

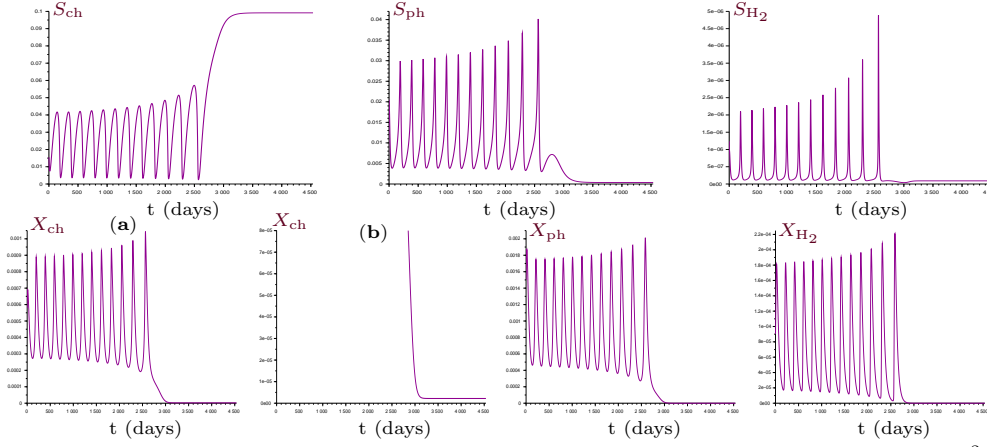


FIG. F.2. Trajectories of S_{ch} , S_{ph} , S_{H_2} , X_{ch} , X_{ph} and X_{H_2} for $S_{ch,in} = 0.0995$ (in kgCOD/m^3): Convergence to the stable steady state SS3. (b) A magnification of (a) showing that the solution of (4.1) converges to the nonzero X_{ch} -component of SS3.

describing the dynamics and facilitate numerical simulations, the following rescaling of the variables was used in [24]:

$$(F.1) \quad \begin{aligned} X_0 &= \frac{X_{ch}}{K_{S,ch}Y_{ch}}, & X_1 &= \frac{X_{ph}}{K_{S,ph}Y_{ph}}, & X_2 &= \frac{X_{H_2}}{K_{S,H_2}Y_{H_2}}, \\ S_0 &= \frac{S_{ch}}{K_{S,ch}}, & S_1 &= \frac{S_{ph}}{K_{S,ph}}, & S_2 &= \frac{S_{H_2}}{K_{S,H_2}}, & \tau &= k_{m,ch}Y_{ch}t. \end{aligned}$$

Then, with these changes of variables the system given in (4.1) reduced to system

$$(F.2) \quad \begin{cases} \frac{dX_0}{d\tau} = (\nu_0(S_0, S_2) - \alpha - k_0)X_0 \\ \frac{dX_1}{d\tau} = (\nu_1(S_1, S_2) - \alpha - k_1)X_1 \\ \frac{dX_2}{d\tau} = (\nu_2(S_2) - \alpha - k_2)X_2 \\ \frac{dS_0}{d\tau} = \alpha(u_0 - S_0) - \nu_0(S_0, S_2)X_0 \\ \frac{dS_1}{d\tau} = \alpha(u_1 - S_1) + \omega_0\nu_0(S_0, S_2)X_0 - \nu_1(S_1, S_2)X_1 \\ \frac{dS_2}{d\tau} = \alpha(u_2 - S_2) - \omega_2\nu_0(S_0, S_2)X_0 + \omega_1\nu_1(S_1, S_2)X_1 - \nu_2(S_2)X_2. \end{cases}$$

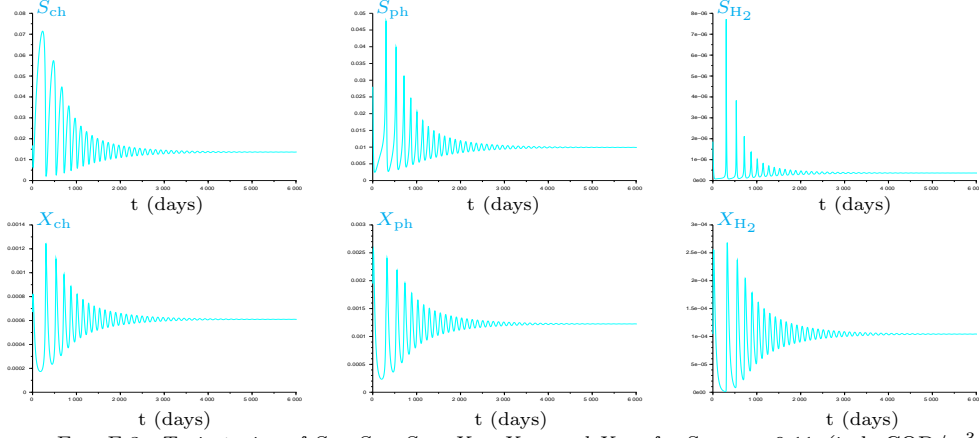


FIG. F.3. Trajectories of S_{ch} , S_{ph} , S_{H_2} , X_{ch} , X_{ph} and X_{H_2} for $S_{ch,in} = 0.11$ (in kgCOD/m^3): Convergence to the positive steady state SS6.

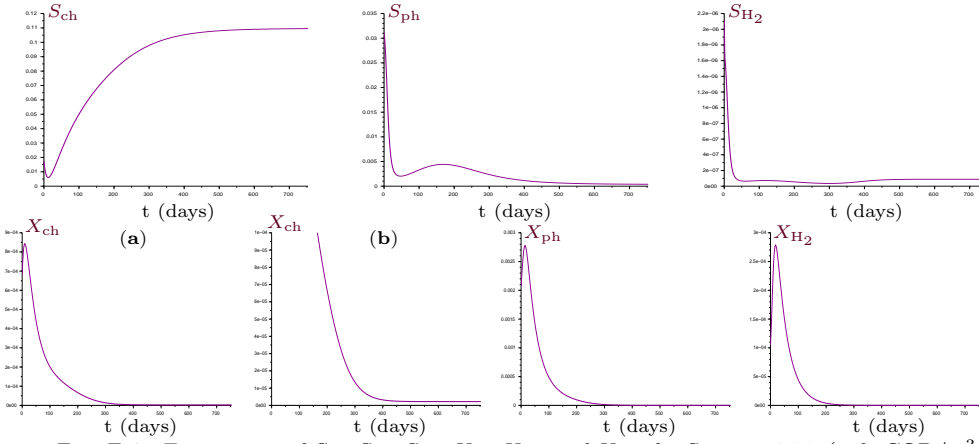


FIG. F.4. Trajectories of S_{ch} , S_{ph} , S_{H_2} , X_{ch} , X_{ph} and X_{H_2} for $S_{ch,in} = 0.11$ (in kgCOD/m^3): Convergence to the stable steady state SS3. (b) A magnification of (a) showing that the solution of (4.1) converges to the nonzero X_{ch} -component of SS3.

The operating parameters are

$$\alpha = \frac{D}{k_{m,ch}Y_{ch}}, \quad u_0 = \frac{S_{ch}^{in}}{K_{S,ch}}, \quad u_1 = \frac{S_{ph}^{in}}{K_{S,ph}}, \quad u_2 = \frac{S_{H_2}^{in}}{K_{S,H_2}}.$$

The yield coefficients are

$$\omega_0 = \frac{K_{S,ch}}{K_{S,ph}} \frac{224}{208} (1 - Y_{ch}), \quad \omega_1 = \frac{K_{S,ph}}{K_{S,H_2}} \frac{32}{224} (1 - Y_{ph}), \quad \omega_2 = \frac{16}{208} \frac{K_{S,ch}}{K_{S,H_2}}.$$

The death rates are

$$k_0 = \frac{k_{dec,ch}}{k_{m,ch}Y_{ch}}, \quad k_1 = \frac{k_{dec,ph}}{k_{m,ch}Y_{ch}}, \quad k_2 = \frac{k_{dec,H_2}}{k_{m,ch}Y_{ch}}.$$

The growth functions are

$$(F.3) \quad \nu_0(S_0, S_2) = \frac{S_0}{1+S_0} \frac{S_2}{K_P+S_2}, \quad \nu_1(S_1, S_2) = \frac{\phi_1 S_1}{1+S_1} \frac{1}{1+K_I S_2}, \quad \nu_2(S_2) = \frac{\phi_2 S_2}{1+S_2},$$

where the biological parameters are given by

$$\phi_1 = \frac{k_{m,ph}Y_{ph}}{k_{m,ch}Y_{ch}}, \quad \phi_2 = \frac{k_{m,H_2}Y_{H_2}}{k_{m,ch}Y_{ch}}, \quad K_P = \frac{K_{S,H_2,C}}{K_{S,H_2}}, \quad K_I = \frac{K_{S,H_2}}{K_{I,H_2}}.$$

The trajectories in Figures 4.4 to 4.6 and F.1 to F.4 were presented according to the variables of model (4.1) using the change of variables (F.1). In Figures 4.4 to 4.6, the projections of the orbits of the six-dimensional phase space into the three-dimensional space $(X_{\text{ch}}, X_{\text{ph}}, X_{\text{H}_2})$ shows the appearance and disappearance of a stable limit cycle for different values of $S_{\text{ch}}^{\text{in}} > \sigma_5$. The plot of the limit cycle was obtained by solving the ordinary differential equations using the default solver “*lsoda*” from the ODEPACK package in Scilab. Tables 12 and 13 present the components of the stable steady states SS3 and SS6, and all the initial conditions chosen to trace the different trajectories of model (4.1) in Figures 4.4 to 4.6 and F.1 to F.4.

TABLE 12

Steady states SS3 and SS6 of model (4.1) corresponding to Figures 4.4 to 4.6 and F.1 to F.4. The biological parameters are provided in Table 14. The operating parameters are $D = 0.01$, $S_{\text{ph}}^{\text{in}} = 0$, $S_{\text{H}_2}^{\text{in}} = 2.67 \times 10^{-5}$ and $S_{\text{ch}}^{\text{in}}$ given in the second column.

Figure	$S_{\text{ch}}^{\text{in}}$	SS3 = $(X_{\text{ch}}, 0, 0, S_{\text{ch}}, S_{\text{ph}}, S_{\text{H}_2})$ SS6 = $(X_{\text{ch}}, X_{\text{ph}}, X_{\text{H}_2}, S_{\text{ch}}, S_{\text{ph}}, S_{\text{H}_2})$
4.4	0.098	$(2.19 \cdot 10^{-6}, 0, 0, 9.77 \cdot 10^{-2}, 3.65 \cdot 10^{-4}, 9.17 \cdot 10^{-8})$ $(5.34 \cdot 10^{-4}, 1.06 \cdot 10^{-3}, 8.80 \cdot 10^{-5}, 1.36 \cdot 10^{-2}, 9.93 \cdot 10^{-3}, 3.62 \cdot 10^{-7})$
4.5 F.1 F.2	0.0995	$(2.19 \cdot 10^{-6}, 0, 0, 9.92 \cdot 10^{-2}, 3.65 \cdot 10^{-4}, 9.12 \cdot 10^{-8})$ $(5.44 \cdot 10^{-4}, 1.08 \cdot 10^{-3}, 9.00 \cdot 10^{-5}, 1.36 \cdot 10^{-2}, 9.93 \cdot 10^{-3}, 3.62 \cdot 10^{-7})$
4.6 F.3 F.4	0.11	$(2.19 \cdot 10^{-6}, 0, 0, 1.10 \cdot 10^{-1}, 3.65 \cdot 10^{-4}, 8.79 \cdot 10^{-8})$ $(6.10 \cdot 10^{-4}, 1.22 \cdot 10^{-3}, 1.04 \cdot 10^{-4}, 1.36 \cdot 10^{-2}, 9.93 \cdot 10^{-3}, 3.62 \cdot 10^{-7})$

TABLE 13

The initial conditions of solutions of model (4.1) in Figures 4.4 to 4.6 and F.1 to F.4 are obtained from the initial conditions of the solutions of model (F.2) by using the change of variables (F.1). The initial conditions of (F.2) are given by $X_i(0) = X_i^* + \varepsilon$ and $S_i(0) = S_i^* + \varepsilon$, $i = 0, 1, 2$ where X_i^* and S_i^* are the components of SS6 and ε is given in the second column. When there is more than one trajectory in the figure, its color is indicated in the first column.

Figure Color	ε	$(X_{\text{ch}}(0), X_{\text{ph}}(0), X_{\text{H}_2}(0), S_{\text{ch}}(0), S_{\text{ph}}(0), S_{\text{H}_2}(0))$
4.4	$9.7 \cdot 10^{-3}$	$(5.44 \cdot 10^{-4}, 1.17 \cdot 10^{-3}, 8.80 \cdot 10^{-5}, 1.42 \cdot 10^{-2}, 1.29 \cdot 10^{-2}, 6.05 \cdot 10^{-7})$
4.5		
Pink	10^{-2}	$(5.54 \cdot 10^{-4}, 1.20 \cdot 10^{-3}, 9.00 \cdot 10^{-5}, 1.42 \cdot 10^{-2}, 1.29 \cdot 10^{-2}, 6.12 \cdot 10^{-7})$
blue	$3.2 \cdot 10^{-2}$	$(5.76 \cdot 10^{-4}, 1.46 \cdot 10^{-3}, 9.00 \cdot 10^{-5}, 1.53 \cdot 10^{-2}, 1.96 \cdot 10^{-2}, 1.16 \cdot 10^{-6})$
Green	$3.5 \cdot 10^{-2}$	$(5.79 \cdot 10^{-4}, 1.50 \cdot 10^{-3}, 9.00 \cdot 10^{-5}, 1.55 \cdot 10^{-2}, 2.05 \cdot 10^{-2}, 1.24 \cdot 10^{-6})$
4.6		
blue	$6 \cdot 10^{-2}$	$(6.71 \cdot 10^{-4}, 1.95 \cdot 10^{-3}, 1.04 \cdot 10^{-4}, 1.68 \cdot 10^{-2}, 2.80 \cdot 10^{-2}, 1.86 \cdot 10^{-6})$
Green	$7 \cdot 10^{-2}$	$(6.81 \cdot 10^{-4}, 2.07 \cdot 10^{-3}, 1.04 \cdot 10^{-4}, 1.74 \cdot 10^{-2}, 3.11 \cdot 10^{-2}, 2.11 \cdot 10^{-6})$
F.1	$2 \cdot 10^{-3}$	$(5.46 \cdot 10^{-4}, 1.10 \cdot 10^{-3}, 9.00 \cdot 10^{-5}, 1.37 \cdot 10^{-2}, 1.05 \cdot 10^{-2}, 4.12 \cdot 10^{-7})$
F.2	$3.5 \cdot 10^{-2}$	$(5.79 \cdot 10^{-4}, 1.50 \cdot 10^{-3}, 9.00 \cdot 10^{-5}, 1.55 \cdot 10^{-2}, 2.05 \cdot 10^{-2}, 1.24 \cdot 10^{-6})$
F.3	$6 \cdot 10^{-2}$	$(6.71 \cdot 10^{-4}, 1.95 \cdot 10^{-3}, 1.04 \cdot 10^{-4}, 1.68 \cdot 10^{-2}, 2.80 \cdot 10^{-2}, 1.86 \cdot 10^{-6})$
F.4	$7 \cdot 10^{-2}$	$(6.81 \cdot 10^{-4}, 2.07 \cdot 10^{-3}, 1.04 \cdot 10^{-4}, 1.74 \cdot 10^{-2}, 3.11 \cdot 10^{-2}, 2.11 \cdot 10^{-6})$

Appendix G. Tables. In this section, the biological parameter values are provided in Table 14. In Table 15, we present the auxiliary functions in the case of the growth functions given by (E.3).

TABLE 14

Nominal parameter values, where $i = \text{ch, ph, H}_2$. Units are expressed in Chemical Oxygen Demand (COD).

Parameters	Nominal values	Units
$k_{m,\text{ch}}$	29	kgCOD _S /kgCOD _X /d
$K_{S,\text{ch}}$	0.053	kgCOD/m ³
Y_{ch}	0.019	kgCOD _X /kgCOD _S
$k_{m,\text{ph}}$	26	kgCOD _S /kgCOD _X /d
$K_{S,\text{ph}}$	0.302	kgCOD/m ³
Y_{ph}	0.04	kgCOD _X /kgCOD _S
k_{m,H_2}	35	kgCOD _S /kgCOD _X /d
K_{S,H_2}	2.5×10^{-5}	kgCOD/m ³
$K_{S,\text{H}_2,c}$	1.0×10^{-6}	kgCOD/m ³
Y_{H_2}	0.06	kgCOD _X /kgCOD _S
$k_{\text{dec},i}$	0.02	d ⁻¹
K_{I,H_2}	3.5×10^{-6}	kgCOD/m ³

TABLE 15

Auxiliary functions in the case of growth functions given by (E.3).

Auxiliary function	Definition domain
$M_0(y, s_2) = \frac{yK_0(L_0+s_2)}{m_0s_2-y(L_0+s_2)}$	$0 \leq y < \frac{m_0s_2}{L_0+s_2}$
$M_1(y, s_2) = \frac{yK_1(K_I+s_2)}{m_1K_I-y(K_I+s_2)}$	$0 \leq y < \frac{m_1K_I}{K_I+s_2}$
$M_2(y) = \frac{yK_2}{m_2-y}$	$0 \leq y < m_2$
$M_3(s_0, z) = \frac{zL_0(K_0+s_0)}{m_0s_0-z(K_0+s_0)}$	$0 \leq z < \frac{m_0s_0}{K_0+s_0}$
$s_2^0(D) = \frac{L_0(D+a_0)}{m_0-D-a_0}$	$D+a_0 < m_0$
$s_2^1(D) = \frac{K_I(m_1-D-a_1)}{D+a_1}$	$D+a_1 < m_1$
$\Psi(s_2, D) = (1-\omega) \frac{(D+a_0)K_0(L_0+s_2)}{m_0s_2-(D+a_0)(L_0+s_2)} + \frac{(D+a_1)K_1(K_I+s_2)}{m_1K_I-(D+a_1)(K_I+s_2)} + s_2$	$\{D \in I_1 : s_2^0 < s_2 < s_2^1\}$
$\psi_0(s_0) = \frac{m_0s_0(s_2^{\text{in}}-\omega(s_0^{\text{in}}-s_0))}{(K_0+s_0)(L_0+s_2^{\text{in}}-\omega(s_0^{\text{in}}-s_0))}$	$s_0 \in [\max(0, s_0^{\text{in}}-s_2^{\text{in}}/\omega), +\infty)$
$\psi_1(s_1) = \frac{m_1s_1K_I}{(K_1+s_1)(K_I+s_2^{\text{in}}+s_1^{\text{in}}-s_1)}$	$s_1 \in [0, s_1^{\text{in}}+s_2^{\text{in}}]$

REFERENCES

- [1] D. Batstone, J. Keller, I. Angelidaki, S. Kalyuzhnyi, S. Pavlostathis, A. Rozzi, W. Sanders, H. Siegrist, and V. Vavilin, *The IWA Anaerobic Digestion Model No 1 (ADM1)*, Water Sci Technol., 45 (2002), pp. 65–73, <https://doi.org/10.2166/wst.2002.0292>.
- [2] B. Benyahia, T. Sari, B. Cherki, and J. Harmand, *Bifurcation and stability analysis of a two step model for monitoring anaerobic digestion processes*, J. Proc. Control, 22 (2012), pp. 1008–1019, <https://doi.org/10.1016/j.jprocont.2012.04.012>.
- [3] O. Bernard, Z. Hadj-Sadok, D. Dochain, A. Genovesi, and J.-P. Steyer, *Dynamical model development and parameter identification for an anaerobic wastewater treatment process*, Biotechnol. Bioeng., 75 (2001), pp. 424–438, <https://doi.org/10.1002/bit.10036>.
- [4] A. Bornhöft, R. Hanke-Rauschenbach, and K. Sundmacher, *Steady-state analysis of the Anaerobic Digestion Model No. 1 (ADM1)*, J. Nonlinear Dyn., 73 (2013), pp. 535–549, <https://doi.org/10.1007/s11071-013-0807-x>.
- [5] A. Burchard, *Substrate degradation by a mutualistic association of two species in the chemostat*, J. Math. Biol., 32 (1994), pp. 465–489, <https://doi.org/10.1007/BF00160169>.
- [6] Y. Daoud, N. Abdellatif, T. Sari, and J. Harmand, *Steady state analysis of a syntrophic model: The effect of a new input substrate concentration*, Math. Model. Nat. Phenom., 13 (2018),

- pp. 1–22, <https://doi.org/10.1051/mmnp/2018037>.
- [7] M. El-Hajji, N. Chorfi, and M. Jleli, *Mathematical modelling and analysis for a three-tiered microbial food web in a chemostat*, *Electron. J. Differ. Equ.*, 255 (2017), pp. 1–13.
- [8] M. El-Hajji, F. Mazenc, and J. Harmand, *A mathematical study of a syntrophic relationship of a model of anaerobic digestion process*, *Math. Biosci. Eng.*, 7 (2010), pp. 641–656, <https://doi.org/10.3934/mbe.2010.7.641>.
- [9] F. Gantmacher, *Application of the theory of matrices*, Interscience Publishers, INC. New York, 2004.
- [10] MAPLE, *version 17.0.0.0*, Waterloo Maple Inc., Waterloo, Ontario, 2018.
- [11] C. Martinez, A. Ávila, F. Mairet, L. Meier, and D. Jeison, *Modeling and analysis of an absorption column connected to a microalgae culture*, *SIAM J. Appl. Math.*, 80 (2020), pp. 772–791, <https://doi.org/10.1137/18M1225641>.
- [12] J. Mata-Alvarez, S. Macè, and P. Llabrès, *Anaerobic digestion of organic solid wastes. an overview of research achievements and perspectives*, *Bioresour. Technol.*, 74 (2000), pp. 3–16, [https://doi.org/10.1016/S0960-8524\(00\)00023-7](https://doi.org/10.1016/S0960-8524(00)00023-7).
- [13] R. May, *Stability and Complexity in Model Ecosystems*, Princeton Univ. Press, NJ., USA, 1973.
- [14] T. Meadows, M. Weeder mann, and G. Wolkowicz, *Global analysis of a simplified model of anaerobic digestion and a new result for the chemostat*, *SIAM J. Appl. Math.*, 79 (2019), pp. 668–689, <https://doi.org/10.1137/18M1198788>.
- [15] S. Nouaoura, R. Fekih-Salem, N. Abdellatif, and T. Sari, *Mathematical analysis of a three-tiered food-web in the chemostat*. hal-02878246, (2020), <https://hal.archives-ouvertes.fr/hal-02878246>.
- [16] P. J. Reilly, *Stability of commensalistic systems*, *Biotechnol. Bioeng.*, 16 (1974), pp. 1373–1392, <https://doi.org/10.1002/bit.260161006>.
- [17] T. Sari, M. El-Hajji, and J. Harmand, *The mathematical analysis of a syntrophic relationship between two microbial species in a chemostat*, *Math. Biosci. Eng.*, 9 (2012), pp. 627–645, <https://doi.org/10.3934/mbe.2012.9.627>.
- [18] T. Sari and J. Harmand, *A model of a syntrophic relationship between two microbial species in a chemostat including maintenance*, *Math. Biosci.*, 275 (2016), pp. 1–9, <https://doi.org/10.1016/j.mbs.2016.02.008>.
- [19] T. Sari and M. J. Wade, *Generalised approach to modelling a three-tiered microbial food-web*, *Math. Biosci.*, 291 (2017), pp. 21–37, <https://doi.org/10.1016/j.mbs.2017.07.005>.
- [20] M. Sbarciog, M. Loccufier, and E. Noldus, *Determination of appropriate operating strategies for anaerobic digestion systems*, *Biochem. Eng. J.*, 51 (2010), pp. 180–188, <https://doi.org/10.1016/j.bej.2010.06.016>.
- [21] SCILAB, *version 6.0.1 (64-bit)*, Scilab Enterprises SAS, 2018.
- [22] S. Sobieszek, G. S. K. Wolkowicz, and M. J. Wade, *A qualitative study of an anaerobic food-web reveals the importance of hydrogen for microbial stability*. arXiv:2002.06057, (2020), <https://arxiv.org/abs/2002.06057>.
- [23] E. I. P. Volcke, M. Sbarciog, E. J. L. Noldus, B. De Baets, and M. Loccufier, *Steady state multiplicity of two-step biological conversion systems with general kinetics*, *Math. Biosci.*, 228 (2010), pp. 160–170, <https://doi.org/10.1016/j.mbs.2010.09.004>.
- [24] M. J. Wade, R. W. Pattinson, N. G. Parker, and J. Dolting, *Emergent behaviour in a chlorophenol-mineralising three-tiered microbial ‘food web’*, *J. Theoret. Biol.*, 389 (2016), pp. 171–186, <https://doi.org/10.1016/j.jtbi.2015.10.032>.
- [25] M. Weeder mann, G. Seo, and G. S. K. Wolkowicz, *Mathematical model of anaerobic digestion in a chemostat: Effects of syntrophy and inhibition*, *J. Biol. Dyn.*, 7 (2013), pp. 59–85, <https://doi.org/10.1080/17513758.2012.755573>.
- [26] M. Weeder mann, G. S. K. Wolkowicz, and J. Sasara, *Optimal biogas production in a model for anaerobic digestion*, *J. Nonlinear Dyn.*, 81 (2015), pp. 1097–1112, <https://doi.org/10.1007/s11071-015-2051-z>.
- [27] A. Xu, J. Dolting, T. P. Curtis, G. Montague, and E. Martin, *Maintenance affects the stability of a two-tiered microbial ‘food chain’?*, *J. Theoret. Biol.*, 276 (2011), pp. 35–41, <https://doi.org/10.1016/j.jtbi.2011.01.026>.